



HAL
open science

Atmospheric Rivers and Weather Types in Aotearoa New Zealand: A two-way story

Benjamin Pohl, Hamish D Prince, Jonathan Wille, Daniel G Kingston,
Nicolas J Cullen, Nicolas Fauchereau

► **To cite this version:**

Benjamin Pohl, Hamish D Prince, Jonathan Wille, Daniel G Kingston, Nicolas J Cullen, et al.. Atmospheric Rivers and Weather Types in Aotearoa New Zealand: A two-way story. *Journal of Geophysical Research: Atmospheres*, 2023, 128 (15), pp.e2022JD037209. 10.1029/2022jd037209 . hal-04179189

HAL Id: hal-04179189

<https://hal.science/hal-04179189>

Submitted on 9 Aug 2023

HAL is a multi-disciplinary open access archive for the deposit and dissemination of scientific research documents, whether they are published or not. The documents may come from teaching and research institutions in France or abroad, or from public or private research centers.

L'archive ouverte pluridisciplinaire **HAL**, est destinée au dépôt et à la diffusion de documents scientifiques de niveau recherche, publiés ou non, émanant des établissements d'enseignement et de recherche français ou étrangers, des laboratoires publics ou privés.



RESEARCH ARTICLE

10.1029/2022JD037209

Benjamin Pohl and Hamish D. Prince
share co-first authorship

Atmospheric Rivers and Weather Types in Aotearoa New Zealand: A Two-Way Story

Benjamin Pohl¹ , Hamish D. Prince² , Jonathan Wille³ , Daniel G. Kingston⁴ ,
Nicolas J. Cullen⁴ , and Nicolas Fauchereau⁵

¹Laboratoire Biogéosciences, UMR6282 CNRS/Université de Bourgogne Franche-Comté, Dijon, France, ²Department of Atmospheric and Oceanic Sciences, University of Wisconsin-Madison, Madison, WI, USA, ³Université Grenoble Alpes/CNRS/IRD/G-INP, IGE, Grenoble, France, ⁴School of Geography, University of Otago, Dunedin, New Zealand, ⁵National Institute of Water and Atmospheric Research, Auckland, New Zealand

Key Points:

- Weather types (WTs) are major drivers of atmospheric rivers (ARs) (frequency, angle, moisture transport direction, and landfalling region)
- ARs explain part of within-type diversity (circulation and rainfall anomalies)
- Combined or separate effects of WTs and ARs strongly vary from one region of Aotearoa New Zealand to another

Supporting Information:

Supporting Information may be found in the online version of this article.

Correspondence to:

B. Pohl,
benjamin.pohl@u-bourgogne.fr

Citation:

Pohl, B., Prince, H. D., Wille, J., Kingston, D. G., Cullen, N. J., & Fauchereau, N. (2023). Atmospheric rivers and weather types in Aotearoa New Zealand: A two-way story. *Journal of Geophysical Research: Atmospheres*, 128, e2022JD037209. <https://doi.org/10.1029/2022JD037209>

Received 30 MAY 2022
Accepted 28 JUL 2023

Author Contributions:

Conceptualization: Benjamin Pohl
Data curation: Benjamin Pohl, Hamish D. Prince, Nicolas Fauchereau
Formal analysis: Benjamin Pohl, Hamish D. Prince, Jonathan Wille, Daniel G. Kingston, Nicolas J. Cullen, Nicolas Fauchereau
Funding acquisition: Benjamin Pohl, Nicolas Fauchereau
Methodology: Benjamin Pohl

© 2023. The Authors.

This is an open access article under the terms of the [Creative Commons Attribution-NonCommercial-NoDerivs](https://creativecommons.org/licenses/by/4.0/) License, which permits use and distribution in any medium, provided the original work is properly cited, the use is non-commercial and no modifications or adaptations are made.

Abstract Here, we analyze the inter-relationships between weather types (WTs) and atmospheric rivers (ARs) around Aotearoa New Zealand (ANZ), their respective properties, as well as their combined and separate influence on daily precipitation amounts and extremes. Results show that ARs are often associated with 3–4 WTs, but these WTs change depending on the regions where ARs landfall. The WTs most frequently associated with ARs generally correspond to those favoring anomalously strong westerly wind in the mid-latitudes, especially for southern regions of ANZ, or northwesterly anomalies favoring moisture export from the lower latitudes, especially for the northern regions. WTs and ARs show strong within-type and inter-event diversity. The synoptic patterns of the WTs significantly differ when they are associated with AR occurrences, with atmospheric centers of actions being shifted so that moisture fluxes toward ANZ are enhanced. The location, angle, and persistence of ARs appear strongly driven by the synoptic configurations of the WTs. Although total moisture transport shows weaker WT-dependency, it appears strongly related to zonal wind speed to the south of ANZ, or the moisture content of the air mass to the north. Finally, WT influence on daily precipitation may completely change depending on their association, or lack thereof, with AR events. WTs traditionally considered as favorable to wet conditions may conceal daily precipitation extremes occurring during AR days, and anomalously dry days or near-climatological conditions during non-AR days.

Plain Language Summary We analyze here how atmospheric rivers (ARs) relate to weather types (WTs), using the case study of Aotearoa New Zealand (ANZ). We show that, for each region of ANZ, ARs tend to occur during different WTs. Generally, for a given region, most ARs form during 3 or 4 main WTs, and these dominant WTs differ from one region to another. These WTs also show different patterns when they are associated with ARs, compared to other days. AR days have atmospheric configurations that are more efficient to direct moisture fluxes toward the coasts of ANZ. Combining both view of regional climate variability is important to understand the drivers of extreme precipitation events.

1. Introduction

Atmospheric rivers (ARs) have been receiving increasing attention from the scientific community (Ralph et al., 2017). According to the Glossary of Meteorology, they consist of “long, narrow, and transient corridor[s] of strong horizontal water vapor transport that is typically associated with a low-level jet stream ahead of the cold front of an extratropical cyclone” (Ralph et al., 2018). AR genesis occurs more frequently over oceans (Guan & Waliser, 2019; Zhu & Newell, 1994), and ARs are a major conveyor belt of moisture toward the continent and land masses [ibid.]. When they reach land, they can bring heavy precipitation: this is especially the case when and where such ARs encounter a land mass with marked topography, which forces the strong moisture flux to ascend.

Because of its insularity (Figure 1a) and sharp topography almost perpendicular to the dominant westerly winds at latitudes where oceans largely prevail, Aotearoa New Zealand (ANZ) is recurrently affected by AR events (Prince et al., 2021a). AR events landfalling in ANZ have been identified as the key drivers for a vast majority of daily rainfall extremes (Reid et al., 2021; Shu et al., 2021), floods (Kingston et al., 2016), and extreme ablation and snowfall (Porhemmat et al., 2021a, 2021b) impacting the mountain glaciers (Little et al., 2019). These extreme flooding events can cause instability in agriculture and hydroelectric power sectors (Dravitzki & McGregor, 2011) while inflicting long-term social harm in rural regions of ANZ (Smith et al., 2011). With ARs

Visualization: Benjamin Pohl, Hamish D. Prince

Writing – original draft: Benjamin Pohl, Hamish D. Prince, Jonathan Wille, Daniel G. Kingston, Nicolas J. Cullen

projected to become more frequent and transport more moisture toward ANZ under climate change (Espinoza et al., 2018), it is crucial to understand the circulation patterns that influence their behavior.

Looking at the synoptic-scale dynamics, the AR life cycle often begins where Rossby wave breaking in the exit regions of mid-latitude jets streams initiates the penetration of troughs into the subtropics, creating a channel for poleward moisture transport (Hoskins et al., 1985). This enhanced poleward transport of heat and moisture increases upper-level latent heat release encouraging vertical motion from increased diabatic heating, which creates downstream negative potential vorticity anomalies (Pfahl et al., 2015). The injection of negative potential vorticity air masses into higher latitudes fuels atmospheric blocking which allows ARs to persist through multiple extratropical cyclone life cycles (Sodemann & Stohl, 2013), while aiding in explosive cyclone deepening (Zhu & Newell, 1994). Therefore, ARs are not necessarily attached to extratropical cyclones, but the two are mutually beneficial to their development and transport (Z. Zhang et al., 2019).

Because they are embedded in the synoptic-scale variability, but also contribute to shape it in return, ARs tend to show preferential associations, and increased probability, when co-occurring with favorable weather patterns (Kingston et al., 2022). Around ANZ, a set of 12 weather types (WTs) based on a clustering of 1,000 hPa geopotential height fields has been developed by Kidson (2000: K2K hereafter) to account for the space-time variability of such synoptic weather patterns. These WTs have been extensively used by the regional climate community, for paleoclimate reconstructions in the Holocene (Ackerley et al., 2011; Lorrey et al., 2007, 2008, 2012) and Little Ice Age (Lorrey et al., 2014), and to analyze climate change projections (Parsons et al., 2014). Significant relationships have been established between these WTs and the Madden–Julian oscillation (Fauchereau et al., 2016), the interdecadal Pacific oscillation (Lorrey et al., 2007), and the Southern Hemisphere large-scale background conditions (Renwick, 2011). At the more local and regional scales, these WTs have been shown to drive daily climate anomalies (K2K; Pohl et al., 2023; Renwick, 2011), seasonal rainfall anomalies (Lorrey et al., 2007), and to modulate ocean wave heights (Coggins et al., 2016) and ocean–atmosphere coupled summer heatwaves (Salinger et al., 2020). Recently, they have been shown to conceal strong within-type variability (Pohl et al., 2021b: P21 hereafter), a given type being associated with atmospheric ridges and troughs highly variable in intensities and locations. These within-type changes are partly driven by large-scale climate conditions, and explain about the same fraction of regional variability as changes in WT occurrence.

Although evidence has been provided (Kingston et al., 2022) that AR occurrence is significantly modified by the 12 WTs of K2K, several questions remain unresolved to date, including (but not restricted to) the following points:

- How WTs influence AR properties (vertically integrated horizontal vapor transport (IVT), main direction/angle of the ARs, persistence, total vapor transport integrated over the whole life cycle of the AR). These descriptors may determine the moisture sources of the ARs, and are very likely to be modulated by the synoptic configurations, as shown for example, by Pohl et al. (2021c) further south for ARs developing over the Southern Ocean and landfalling in East Antarctica.
- WT patterns may differ when they co-occur versus when they do not co-occur with AR events. Part of the strong within-type diversity linked to changes in the location and intensities of atmospheric centers of action (ACAs: P21) could partly relate to the development (or lack thereof) of ARs in the ANZ sector.
- Although WT influence has been extensively assessed (K2K; Lorrey et al., 2007; Pohl et al., 2023; Renwick, 2011), their separate and combined influence with ARs on daily precipitation amounts, including extremes, remains to be determined. The picture of precipitation changes from one WT to another could be strongly modified depending on their co-occurrence (or lack thereof) with ARs.
- Finally, it seems important to assess how these results change from one region of ANZ to another, depending on the latitude, terrain exposure, local climate, coastline/land-sea contrasts and topography. This is expected to be particularly interesting for ANZ considering previously documented substantial regional differences in AR occurrence and characteristics (Kingston et al., 2022; Prince et al., 2021a) and unusual situation of land-falling ARs occurring on both windward and leeward coasts relative to the prevailing large-scale circulation.

This paper aims at filling these gaps, and proposes therefore to analyze the inter-connections between ARs, WTs and precipitation amounts across ANZ. Both ARs and WTs are considered not only in terms of (co-)occurrence, but also through their properties, as inferred by the set of descriptors respectively proposed by Guan and Waliser (2019) and P21. Daily precipitation fields are derived from a 5-km resolution interpolated product

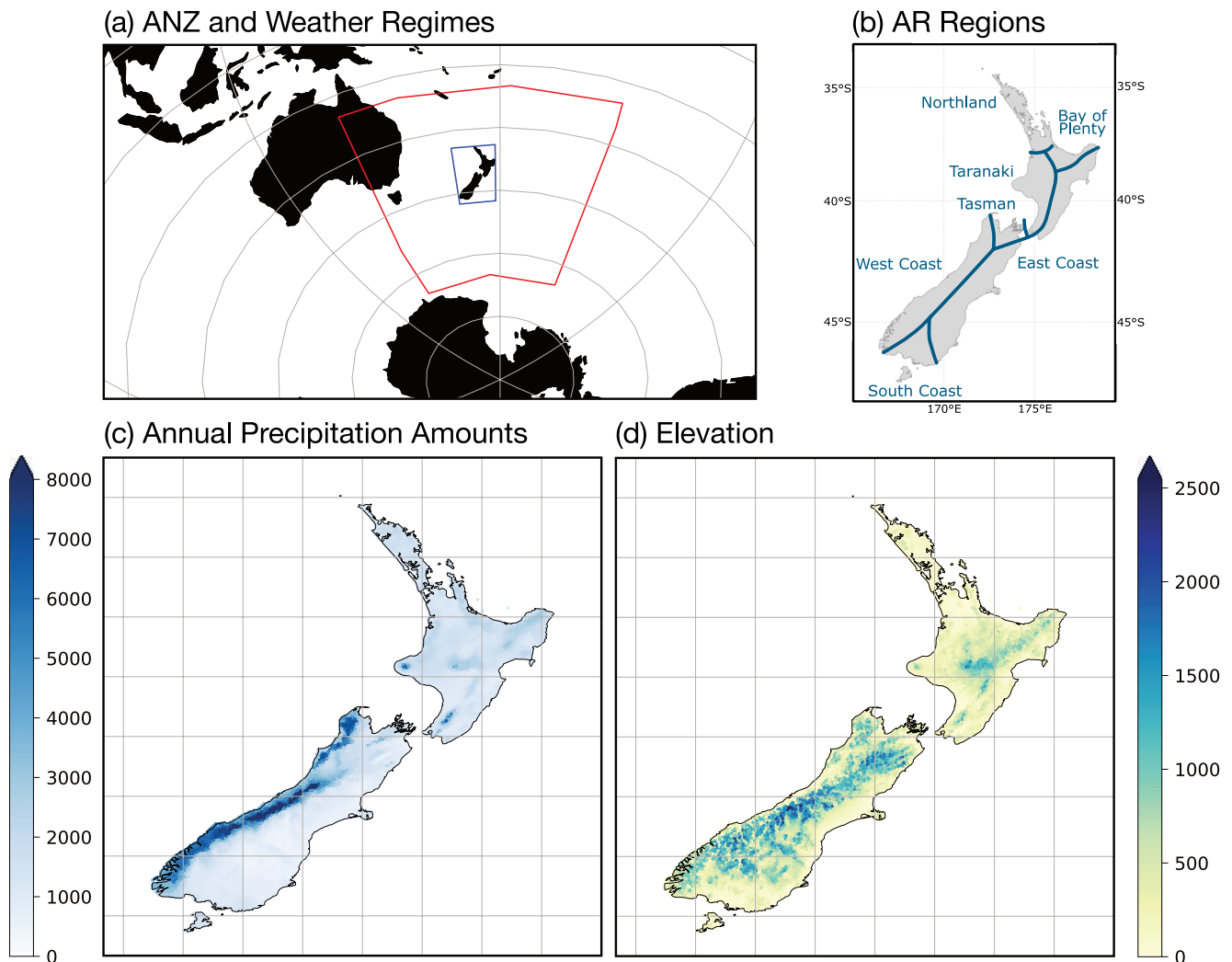


Figure 1. Domain locations, local climate and topography around Aotearoa New Zealand (ANZ). (a) Location of ANZ and domain boundaries used to analyze weather types and their atmospheric centers of action (in red), and local precipitation anomalies in ANZ (in blue). (b) Location of the seven groups of ERA5 grid-points used for atmospheric river analysis. (c) Climatological mean annual precipitation amounts (mm) according to Virtual Climate Station Network data, period 1979–2019. (d) Elevation (m above sea level).

constrained by observational networks, that allows for a detailed analysis of terrain influence on the spatial distribution of daily amounts.

In the following, Section 2 presents the data and methods used in this work. Section 3 presents the AR count in each region of ANZ, and their association with WTs. Section 4 next focuses on their separate versus combined influences on daily precipitation, considering both anomalies and daily extremes. Section 5 addressed the co-occurrence of ARs and WTs, how they change from one part of ANZ to another, and assesses to which extent their intrinsic properties are interdependent. Finally, Section 6 summarizes and discusses our main results.

2. Data and Methods

2.1. Data

Atmospheric fields used here are taken from the ERA5 ensemble reanalysis (Hersbach et al., 2020). ERA5 is the fifth generation of atmospheric reanalysis released by the European Center for Medium-Range Weather Forecasts. It currently covers the period 1979 onward (with an extension to 1950 but with weaker constraint by assimilation due to the lack of satellite data) and includes a 10-member ensemble to quantify uncertainties associated

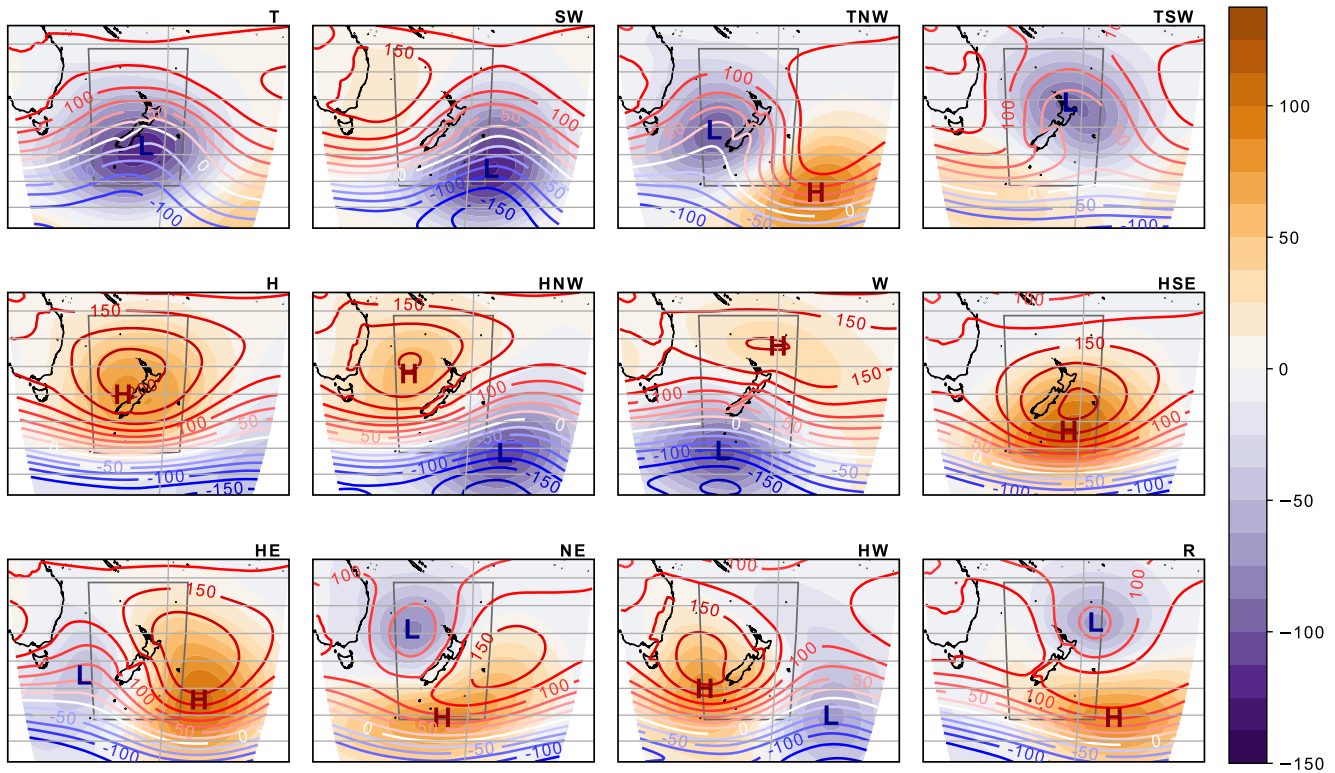


Figure 2. Geopotential height at 1,000 hPa (m) associated with the 12 weather types (WTs) of Kidson (2000). Contours show composite mean Z1000 fields, colors show corresponding Z1000 anomalies. Geopotential heights are derived from ERA5 for the period 1979–2019. Only anomalies that are statistically different from the climatology according to a one-tailed t test at the 95% level are represented. The inner rectangle represents the original domain used by Kidson (2000). Letter H indicates local maximum Z1000 anomalies; L indicates local minimum Z1000 anomalies. ERA5 definition of WT is used. Each WT is labeled with a descriptor that is used for referencing throughout the manuscript.

with the density and quality of the assimilated data. In this work, we use the regular $0.25^\circ \times 0.25^\circ$ grids for daily or 6-hourly fields of geopotential height at 1,000 hPa (m, Z1000) and 700 hPa (Z700) and horizontal wind at 700 hPa (m s^{-1}), and vertically-integrated moisture transport (IVT: $\text{kg m}^{-1} \text{s}^{-1}$) over the period 1979–2019.

Daily precipitation data for ANZ come from the National Institute of Water and Atmospheric Research (NIWA) Virtual Climate Station Network (VCSN). Data coverage for the NIWA VCSN (Tait & Turner, 2005; Tait et al., 2006, 2012) is available from 1972 to present for 13 daily climate variables on a 5×5 km grid covering the country. The approach to generate the NIWA VCSN uses a thin-plate smoothing spline model for spatial interpolation between in situ station data, incorporating two location variables (latitude and longitude) and a third “pattern” variable. For precipitation (Figure 1c), a digital version of an expert-guided 1951–1980 mean annual rainfall isohyet map was used as the pattern variable as a way to represent orographic influences that arise from prevailing circulation interacting with mountainous terrain (Figure 1d). Although they have been successfully used in many previous studies that confirmed their overall good quality, VCSN data yield potentially biased estimates of precipitation, especially in the most elevated parts of the country where the density of rain-gauge and weather stations is much reduced (Jobst et al., 2018; Mason et al., 2017; Tait et al., 2012).

2.2. Methods

As in P21, this study uses the WT classification performed by K2K over the ANZ sector (Figure 2). The corresponding 12 WTs, originally based on 12-hourly maps of Z1000 derived from NCEP/NCAR reanalyses (Kalnay et al., 1996), are updated here using ERA5 daily ensemble fields. Two WT time distributions are therefore considered, the original WT classification based on NCEP/NCAR timing, and the redefined distribution obtained by ascribing each day of each member based on ERA5, over the period 1979–2019, to its nearest type centroid. These two type definitions are seen to differ, with roughly 35% of the days of the period not being ascribed to the

Table 1

Overview of the Internal Descriptors Used for Each of the 12 Weather Types (WTs) Seen in Figure 1 (in Rows), With Their Usual Abbreviations and Their Long Names After Ackerley et al. (2011) and Cullen et al. (2019)

	Low (trough)			High (ridge)			Gradient (trough and ridge)			Grad
	Lat	Lon	Min _Z	Lat	Lon	Max _Z	Diff _{Lat}	Diff _{Lon}	Diff _Z	
T (Trough)	x	x	x							
SW (Southwesterly)	x	x	x							
TNW (Trough Northwesterly)	x	x	x	x	x	x	x	x	x	x
TSW (Trough Southwesterly)	x	x	x							
H (High)				x	x	x				
HNW (High to the Northwest)	x	x	x	x	x	x	x	x	x	x
W (Westerly)	x	x	x	x	x	x	x	x	x	x
HSE (High to the Southeast)				x	x	x				
HE (High to the East)	x	x	x	x	x	x	x	x	x	x
NE (Northeasterly)	x	x	x	x	x	x	x	x	x	x
HW (High to the West)	x	x	x	x	x	x	x	x	x	x
R (Ridge)	x	x	x	x	x	x	x	x	x	x

Note. “Low” columns are for troughs, “High” columns for ridges, and “Gradient” columns for weather types showing both troughs and ridges. Descriptors depict the spatial coordinates (Lat, Lon) and intensities (Min_Z, Max_Z) of the corresponding atmospheric centers of action, and for gradient types, their differences (Diff_{Lat}, Diff_{Lon}, Diff_Z). Grad corresponds to the geopotential height gradient between both centers of action (Diff_Z/distance separating opposite centers of action).

same WT. However, the composite mean fields are very similar, because day swaps between types are associated with similar patterns that differ only in the location of ACAs. The latter are expected to be more precisely defined by ERA5 data due to its much higher spatial resolution. Except when otherwise indicated, all results and conclusions discussed below can be obtained with both WT distributions. More details and a comparison between both WT timings are given in P21.

In addition to the partitioning into 12 discrete WTs, we reuse here the descriptors from P21 that monitor the location and intensity of the main ACAs associated with each type. These descriptors are derived from Z1000 daily anomalies (noted Z1000'), after removing the mean annual cycle, and are calculated over the larger domain shown in Figure 1a. Three groups of WTs are formed, depending on the presence or absence of regional extremes of Z1000' (P21; Table 1). The “Low” group has only one such extreme, consisting of a regional minimum of Z1000' denoting an atmospheric trough. Conversely, the “High” group only includes a regional maximum of Z1000', indicative of an atmospheric ridge. The “Gradient” group has both extremes. The descriptors defined in P21 qualitatively differ from one group of WTs to another. For the “Low” group, three metrics depict the intensity of the low, corresponding to the minimum Z1000' value within the whole domain (Min_Z), and its corresponding latitude and longitude (Lat, Lon) that define its location. The “High” types use the same metrics, but applied to the Z1000' maximum to define the high ACA. The “Gradient” types use both metrics, with additional ones used to depict the relative position and differences between both ACAs. This provides the difference between Z1000' maximum and minimum (Diff_Z), the latitudinal and longitudinal differences in their locations (Diff_{Lat}, Diff_{Lon}), and finally the slope of the geopotential height gradient, defined as $Grad = Diff_{Z'} / \sqrt{Diff_{Lat}^2 + Diff_{Lon}^2}$. All descriptors are quantitative and thus help address one of the main weaknesses of the WT approach, which is in discretizing naturally continuous climate variability (P21).

The AR catalog is taken from the Atmospheric River Tracking Method Intercomparison Project (ARTMIP) Tier 2 reanalysis intercomparison project (Marquardt Collow et al., 2022). We use here the catalog based on the Guan and Waliser (2019) Tracking ARs Globally as Elongated Targets (tARget, algorithm, version 3. AR occurrence is assessed for each grid cell individually and the passage of each AR object (over multiple timesteps) is considered both as a series of contiguous timesteps, and as one event with the day of maximum IVT (Prince et al., 2021b), depending on the AR variables (Table 2). AR objects are detected from ERA5 reanalysis (Hersbach et al., 2020) between 1979 and 2019 (40 years) using hourly IVT at 0.25° resolution. These ARs have been compared to the AR catalog used in Prince et al. (2021a) and results revealed very weak reanalysis-dependency (e.g., Figure

Table 2
Overview of the Atmospheric River (AR) Metrics Given by the Guan and Waliser (2019) AR Detection Algorithm That Are Analyzed in This Work

For each AR timestep	Units
AR_IVTx	$\text{kg m}^{-1} \text{s}^{-1}$
AR_IVTy	
AR_IVTmag	
AR_IVT_direction	$^{\circ}$
For each AR event (sequence of consecutive timesteps)	
Max_IVT	$\text{kg m}^{-1} \text{s}^{-1}$
Max_IVTx	
Max_IVTy	
Max_direction	$^{\circ}$
Duration	hr
Storm_total_IVT	$\text{kg m}^{-1} \text{s}^{-1}$

Note. The first category of metrics is given for each timestep associated with an AR event, while the second category is a statistics calculated over the whole duration (all timesteps included) of the AR event. Units are given by the third column.

S1c in Supporting Information S1): all conclusions given below are qualitatively similar according to these two generations of reanalyses. For illustration purposes, Figure 3a shows two examples of landfalling ARs, reaching the opposite regions (West and East coasts) of the South Island.

The characteristics of the ARs are used throughout this study, specifically the magnitude of the moisture flux in the meridional and zonal direction, the duration of the event, and the maximum total moisture flux throughout the event (Table 2). The relatively narrow landmass New Zealand, situated in the midlatitudes, allows for ARs to make landfall on all coastlines (Prince et al., 2021a). This setup is unique and requires additional consideration, especially when considering ARs that may cause impacts on the eastern side of the country (Prince et al., 2021a). To account for the landfalling direction of the AR, only ARs which have IVT directed from the ocean onto land are considered (a restriction which is discussed below). This leads to the exclusion of many ARs that pass over the eastern side of the country since they made landfall on the western coast and passed over the Southern Alps, rather than making landfall on the east coast. This technique is an extension of the Guan and Waliser (2015) landfall detection which identifies the landfall location based on the presence of ocean upwind of where an AR intersects a coastline, however our method considered for each grid cell individually here rather than for the entire AR object.

The deterministic member of ERA5, available at a 0.25° resolution, describes the coastlines of ANZ with 157 grid-points, materializing all potential landfalling locations for ARs. Although we performed systematically all analyses for all these grid-points, we chose to regroup them below into coherent and homogeneous regions, which were determined by the orientation of the coastline (see Figure S1 in Supporting Information S1 for details). In the remainder of this study, we merely discuss these seven coherent regions (shown in Figure 1b), and provide more detailed explanations and analyses for the West Coast region of the South Island (where ARs are the most severe, due to the topographic forcing of the Southern Alps), and the two most contrasted regions of the country (the South Coast and the Northland regions), which allows us to consider most of the diversity in ARs themselves, and their relationships with the regional WTs.

3. Co-Occurrence Between Atmospheric Rivers and Weather Types

Figure 3 presents the contribution of the detected ARs to moisture transport reaching the ANZ coasts, as a function of IVT. Figure 3d quantifies AR contribution to overall moisture transport, depending on the IVT values. AR are found to occur on average about 11.6% of the time. They contribute to 62% of the moisture transport days for IVT values of $250 \text{ kg m}^{-1} \text{ s}^{-1}$ (a threshold often used in the AR community, including the AR scale of Ralph et al., 2019). The relative importance of ARs further increases for larger IVT values: 94% of the days with an IVT exceeding $500 \text{ kg m}^{-1} \text{ s}^{-1}$ do correspond to AR events. Hence, ARs (as detected by the Guan & Waliser, 2019 algorithm) appear, by far, as the predominant feature that drives moisture advections toward ANZ. While this conclusion is verified for all coastal regions of ANZ, absolute values of IVT may strongly differ, especially between the opposite (West and East) coasts (Figure 3d). Nonetheless, the statistical distribution of IVT (Figures 3b and 3c) confirm that ARs exhibit a statistical distribution of IVT that strongly differs from other days, even when considering these regional differences. Thus, the 10% top ARs, whatever their landfalling location in ANZ, are associated with IVT values that completely differ from those found during NoAR days (Figures 3b and 3c), thereby highlighting that AR have a very specific signature in terms of moisture transport toward ANZ.

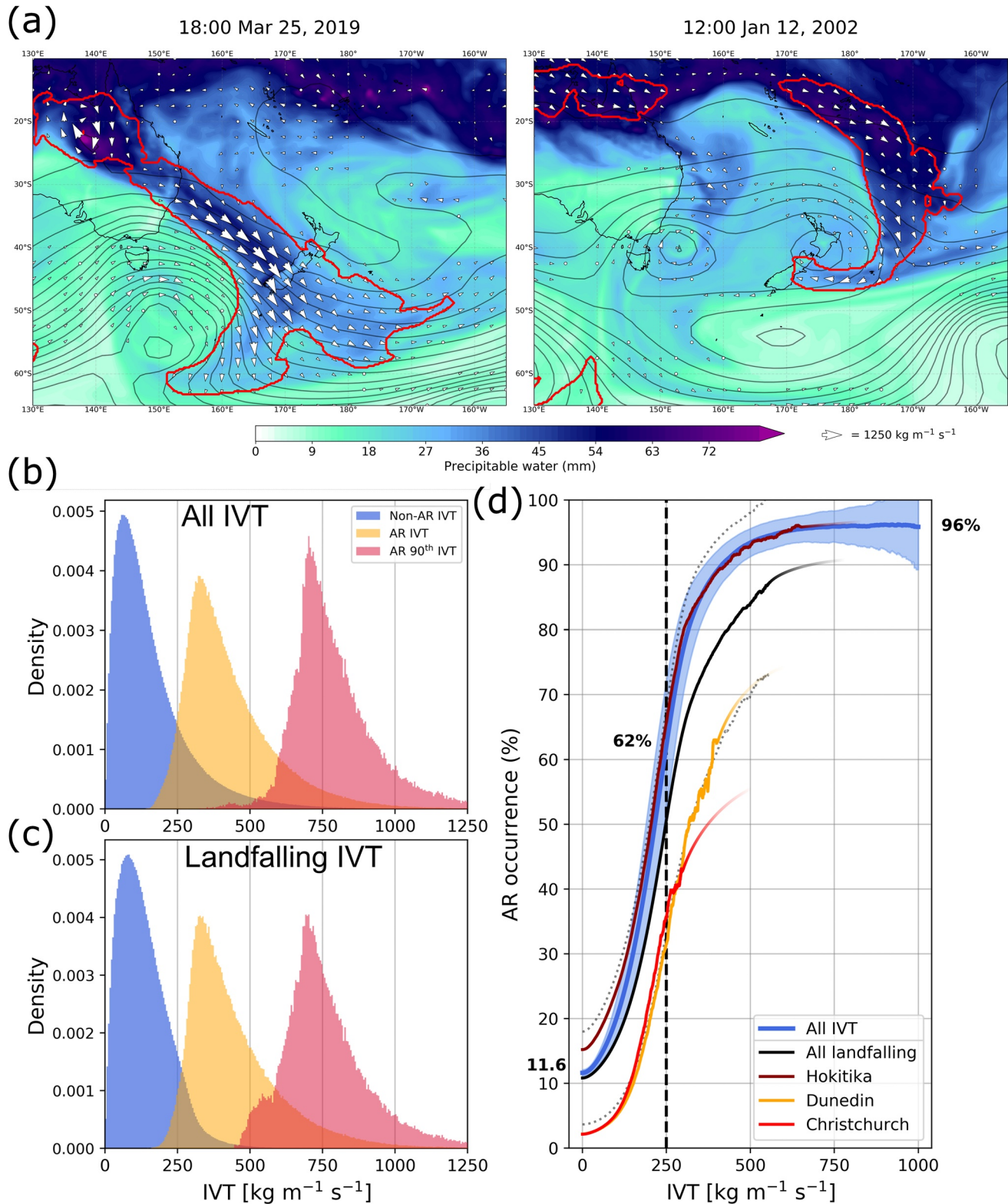


Figure 3. Contribution of atmospheric rivers (ARs) to moisture transport in Aotearoa New Zealand (ANZ). (a) Two examples of landfalling ARs, in the West Coast (left) and East Coast (right) regions of ANZ. Arrows represent vertically-integrated moisture transport ($\text{kg m}^{-1} \text{ s}^{-1}$) and colors represent precipitable water (mm; see color scale). (b, c) Histograms of IVT ($\text{kg m}^{-1} \text{ s}^{-1}$) for non-AR days (blue), landfalling AR days (yellow) and top 10% IVT AR days (red). (d) Contribution of AR days to moisture transport, as a function of IVT. The threshold of $250 \text{ kg m}^{-1} \text{ s}^{-1}$ often used in AR detection schemes is indicated in the figure. The case of Hokitika (West Coast region), Dunedin and Christchurch (East Coast region), are shown to illustrate regional dependency.

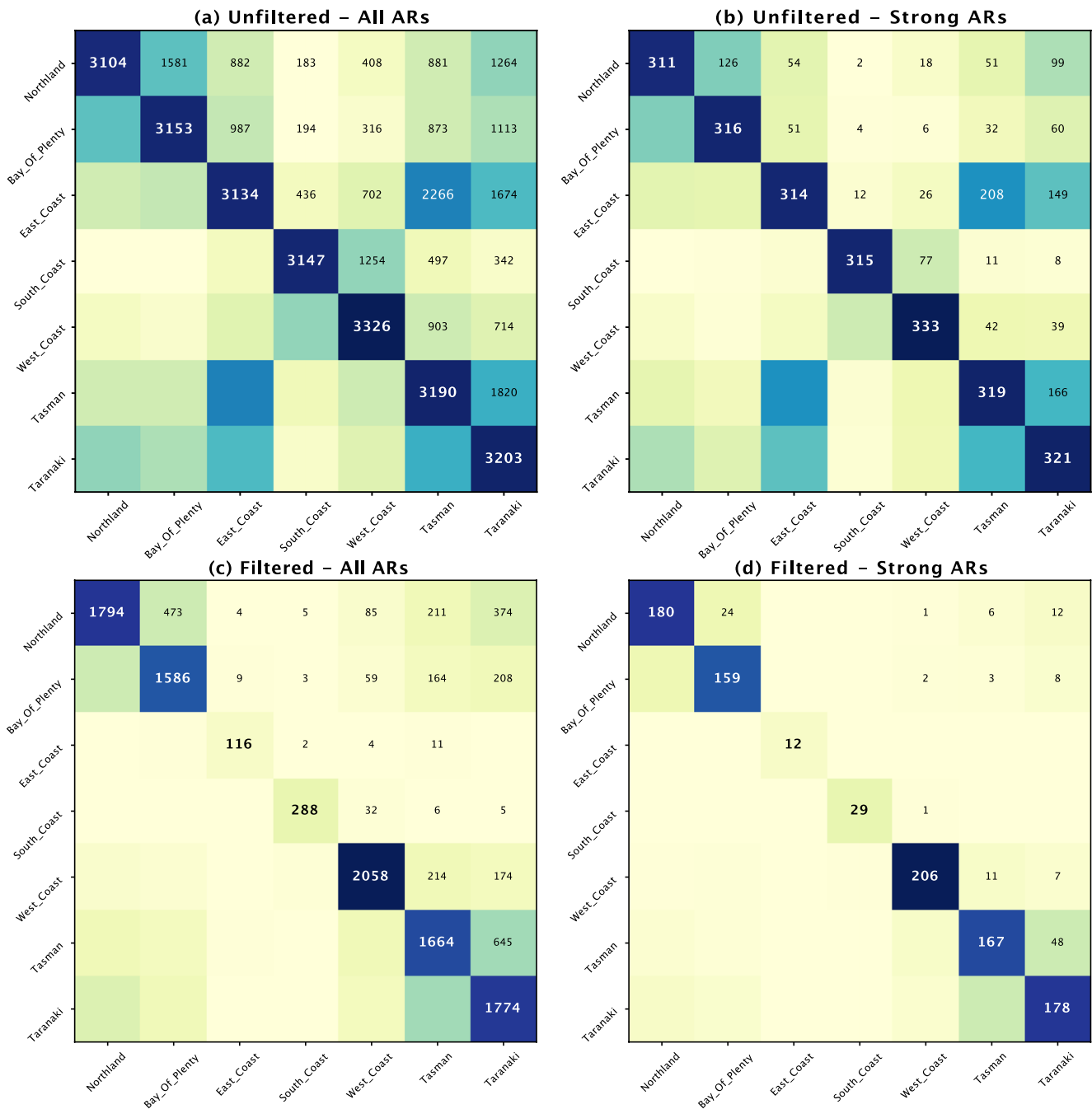


Figure 4. Co-occurrence of atmospheric river (AR) across regions (a: all ARs reaching ANZ; b: 10% strongest ARs according to the Max_IVT descriptor; c: filtered ARs of all IVT but retaining those coming from open sea; d: filtered top 10% ARs). The named regions (groups of grid-points) are shown in Figure 1b. Diagonal: number of days identified as ARs for region, period 1979–2019. Other cells: number of days identified as ARs co-occurring in the two corresponding regions.

Next, we assess the relationship between synoptic WTs and AR occurrence. The seasonality in these relationships and in AR activity is shown and discussed in Supporting Information S1 (Figures S2 and S3). ARs tend to be more frequent during the austral summer season for most parts of ANZ (and this tendency becomes increasingly clear toward the north of the country), but there are more ARs during the winter season for its southern regions. However, the association between ARs and WTs appears weakly modulated by the annual cycle.

Figure 4 shows the number of daily AR detections for each of the seven regions describing the coastlines of ANZ (Figure 1b), and co-detections when ARs hit more than one region. These results first show the dramatic

change in AR occurrence found, for some region, when filtering those ARs that do not reach the corresponding landfalling locations from the open sea (Section 2.2). This is especially true for the eastern and southern parts of ANZ, often embedded in ARs landfalling along the West Coast, and leading to major intrusions of moist air inland according to ERA5. In most cases, however, the topographic barriers of the Alps (Figure 1d) acts to block, or dramatically weaken, the influence of ARs on their leeward side. Once filtered, these results confirm those of Prince et al. (2021a), who depict very few events landfalling over the eastern coasts of both islands (as did for instance a strong AR event in May 2021 that causes heavy rainfall and floods in these relatively flat regions). This contrasts with the frequent AR detections in the northern and western parts of the country, where the combined influence of land-sea contrasts, topographic forcings and moisture transport, enhance the influence of ARs on local precipitation (Kingston et al., 2016; Reid et al., 2021; Shu et al., 2021).

Other values (out of the diagonals) in Figure 4 show the count of AR days co-occurring in the two corresponding regions. Results show that co-detected AR events can be quite frequent for several groups of grid-points, especially for the neighboring regions of Tasman and Taranaki on the one hand, and Northland and Bay of Plenty on the other hand. Figure S1 in Supporting Information S1 shows the co-detection of landfalling ARs for all 157 grid-points of ERA5 describing the ANZ coastlines, and shows that ARs generally tend to be recorded at numerous grid-points simultaneously. In general, the seven regions defined and used here identify the main groups of similar grid-points, where ARs are likely to landfall. The filtering performed in Figure 4 implies that there are very few events that co-occur in grid-points with contrasted terrain exposure (i.e., orientation of the coastline: for instance, the opposite coasts of the South Island). The few events landfalling on the eastern parts of ANZ also seem to show weaker co-variability between adjacent grid-points (Figure S1a in Supporting Information S1), suggesting smaller AR sizes. Finally, the strongest AR events also tend to show weaker co-occurrence, proportionally (Figure 4d). This could denote a more channeled moisture flux, hence the larger values of IVT.

Previous studies already analyzed the association between ARs and the 12 WTs obtained by K2K (Cullen et al., 2019; Kingston et al., 2022; Porhemmat et al., 2021a). However, they mostly considered the AR events leading to major snowfall/ablation or floods. Therefore, previous work mainly focused on the Southern Alps region, where AR development is most frequent (Figure 4c; Prince et al., 2021a; Marquardt Collow et al., 2022). A general assessment of the association between AR occurrence and WT, and how these relationships vary from one region of ANZ to another, remains to be established. This is the aim of Figure 5. Here, we consider the original definition of the WTs, following the work of K2K and based on NCEP/NCAR reanalyzes, but also their redefinition using ERA5 higher-resolution data (P21). This is because both methodologies led to non-negligible differences (roughly 35% of the days being ascribed to a different WT on period 1979–2019), hence the need to characterize the reanalysis-dependency of our conclusions.

Our results first confirm the main conclusions obtained in the aforementioned studies. For the western but also most of the northern parts of ANZ, most AR events occur during the T type, which consists in a low-pressure system located over, on average, south of ANZ, and favoring enhanced westerly winds north of the trough (Figure 2). Thus, this type is generally associated with enhanced westerly winds. It is likely to be associated with AR events for all regions of ANZ considered in Figure 5, albeit its very variable importance from one grid-point to another.

The relationships between ARs and WTs are even more region-dependent for all other WTs. Generally speaking, AR events landfalling in any region of ANZ tend to occur more frequently during the WTs that act to direct atmospheric fluxes and circulation toward that particular region. This is for instance the case for type W (broadly similar to T but shifted to the south: Figure 2) over the western parts of the country, HNW and SW (both favoring southerly anomalies) for the southernmost regions, or TNW (favoring northwesterly anomalies over the north of ANZ: Figure 2) for the northernmost ones (Figure 5) or HE (broadly similar but with ACAs shifted toward the south) for the grid-points aligned along the west coasts of the islands. These side oppositions are, logically, less marked when AR events are not filtered depending on their angle (Figure 4).

Figure 5 also confirms that the original NCEP/NCAR definition of the WTs and their ERA5 redefinition sensibly differ. The case of type W, already identified as associated with large reanalysis-dependency in P21, can also be mentioned here and leads to dissimilar WT contributions to AR occurrences, especially in the West Coast and Tasman regions (i.e., western ANZ: Figure 5). Other non-negligible differences can be found with types NE (e.g., Northland and East Coast), SW (South Coast) or TSW (East Coast), while the other types showing strong dissimilarities between both reanalyzes (e.g., H and HW: P21) being more rarely associated with AR development.

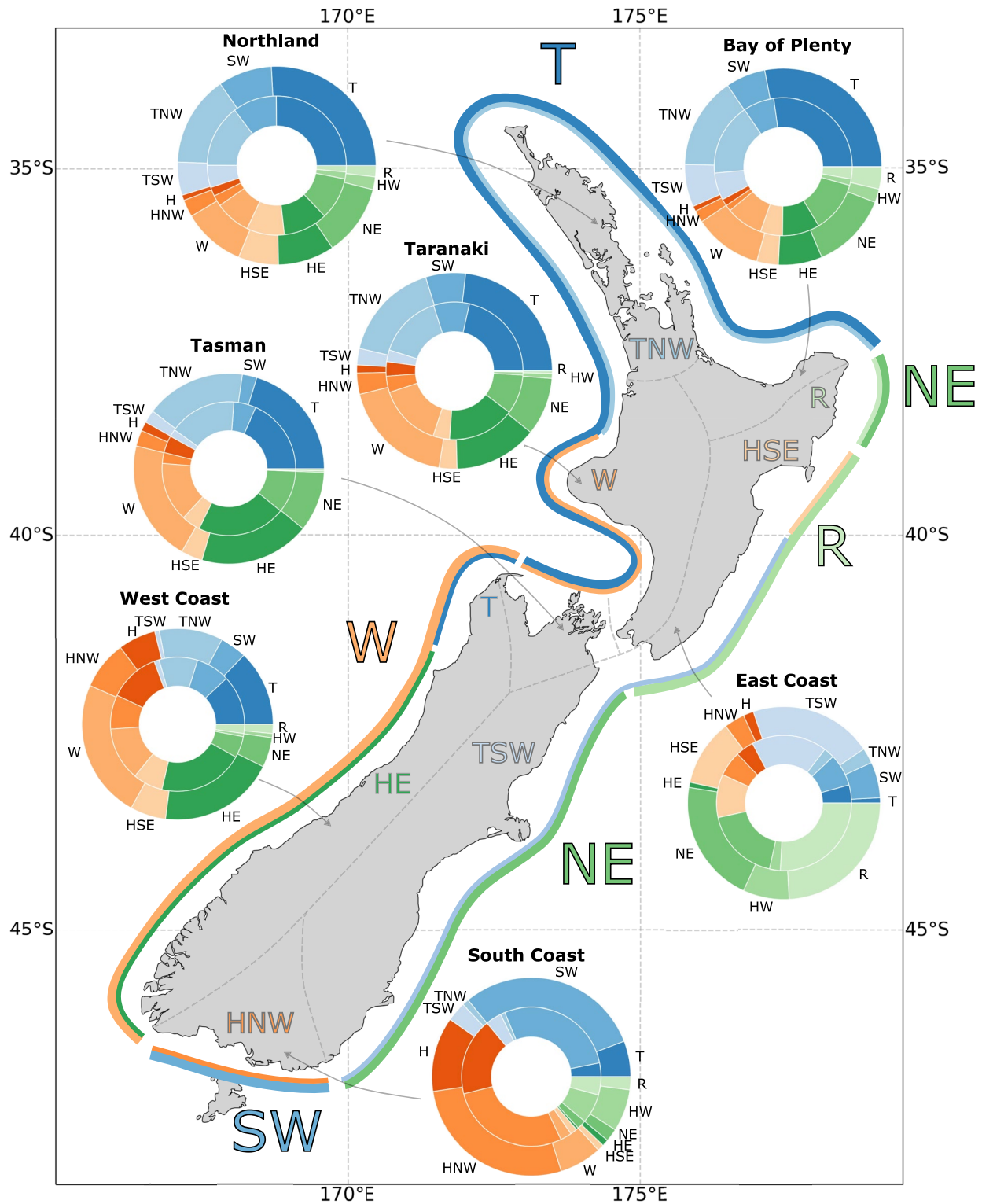


Figure 5. Atmospheric river (AR) occurrence by Kidson type for each region of Aotearoa New Zealand (as shown in Figure 1b), period 1979–2019. Outer pie plots: ERA5 redefinition of Kidson types; inner pie plot: original NCEP distribution. The number of AR days included in each pie plot is given in the diagonal of Figure 4c. The 12 colors in the pie plots correspond to the 12 weather types. The arrows show the location of the central grid-point of each group of grid-points, used in the analyses to analyze AR activity within each region (see Supporting Information S1 for details).

Finally, another major result shown in Figure 5 is that, in all regions of ANZ, AR events are likely to occur during very different synoptic configurations, as materialized here by the WTs. The largest contribution of a given WT is 30.9% (for the HNW type in the South Coast region), showing that the most favorable type is, at best, only responsible for a third of all AR events occurring in a given region. Hence, ARs landfalling in any part of ANZ can result from very different and diverse synoptic types, and these types differ from one region of ANZ to another. The main common result across all regions is that WTs promoting stronger onshore winds are those generally favoring the largest AR occurrences.

4. AR and WT Combined and Separate Influences on Precipitation

4.1. Precipitation Anomalies

The effects of landfalling ARs on precipitation in ANZ has already been assessed before (Reid et al., 2021; Shu et al., 2021), as have been those of WTs (K2K; Pohl et al., 2023; Renwick, 2011). Here, we attempt to consider how their respective influences combine, that is, we analyze precipitation anomalies by WT and depending whether or not these WT days also correspond to AR occurrences. This could contribute to explain part of their strong internal variability, as pointed out by P21. Unlike previous work, we base our analyses on the 5-km resolution VCSN product, thereby allowing for a more detailed and precise assessment of the spatial coherence of rainfall variability patterns associated with WTs and ARs.

Figure 6 shows the daily precipitation anomalies during the five WTs most favorable to AR development (Figure 5), during all days ascribed to the corresponding WT, and then by differentiating NoAR days from AR days. The latter are further separated into two groups, by considering the case of the particularly strong AR events (corresponding to the top 10% ARs according to their associated IVT). Here, the case study retained is the West Coast of the South Island of ANZ (Figures 1b and 5), identified as the region where ARs are responsible for the largest rainfall amounts, and may cause significant damage and environmental impacts (Prince et al., 2021a; Shu et al., 2021). Very similar results (not shown) are obtained, for the corresponding most AR-favorable WTs, in other groups of coastal grid-points across ANZ, which correspond to other possible landfalling locations for ARs (with different exposure due to the geometry of the coastline: Figure 1b).

Results (Figure 6, first column) reveal very strong differences in precipitation anomalies, from one type to another, thereby corroborating previous work (K2K; Jiang et al., 2013; Pohl et al., 2023; Renwick, 2011). Most WTs favorable to AR landfall along the West Coast are associated, on average, with wet anomalies there. The only exception is the HNW type, which recurrently co-occurs with ARs (especially according to the ERA5 redefinition of the WTs: see Figure 5) and tends yet to correspond, on average, to near-climatological daily rainfall west of the main divide. In other regions of ANZ, these regimes produce precipitation anomalies of much weaker amplitude, but of contrasted sign (e.g., drier than normal over the North Island for types W and HE, while the reversed sign prevails along the western slopes of the main reliefs for types T and TNW).

This average picture of WT influence on precipitation anomalies conceals strong internal variability, part of which can be related to AR development. The same WTs, when they do not co-occur with AR events, are indeed related to generally drier conditions over ANZ, and more particularly along the West Coast region (Figure 6, second column). Wet anomalies are weakened for types W, T, and TNW (when not accompanied by any AR). Type HNW, associated with near-normal conditions on average, is even accompanied by marked and significant dry anomalies across ANZ, and more particularly along the West Coast, when no AR development occurs. In sharp contrast, the same five types all show much wetter conditions, especially over the West Coast, during AR landfall (third column), and the wet conditions recorded there are even larger during the 10% strongest AR events (except for HNW; fourth column). Hence, AR occurrence is a key parameter to consider to explain the internal diversity of precipitation amounts within each WT. This result shows that within-type diversity cannot be considered as negligible, when analyzing daily precipitation across ANZ (Pohl et al., 2023).

Although these general conclusions are qualitatively verified for all grid-points around ANZ, the magnitude of the differences between AR and NoAR days is much reduced, quantitatively, over most other regions of the country. This is because precipitation amounts and variability is largest over the West Coast, owing to its sharp topographic barrier almost perpendicular to the dominant westerly winds. Other regions may also show weaker spatial coherence in the precipitation anomaly fields linked to WT and AR occurrences. In the Supporting Information S1, we discuss this issue for the southernmost and northernmost regions of ANZ, retained as case studies.

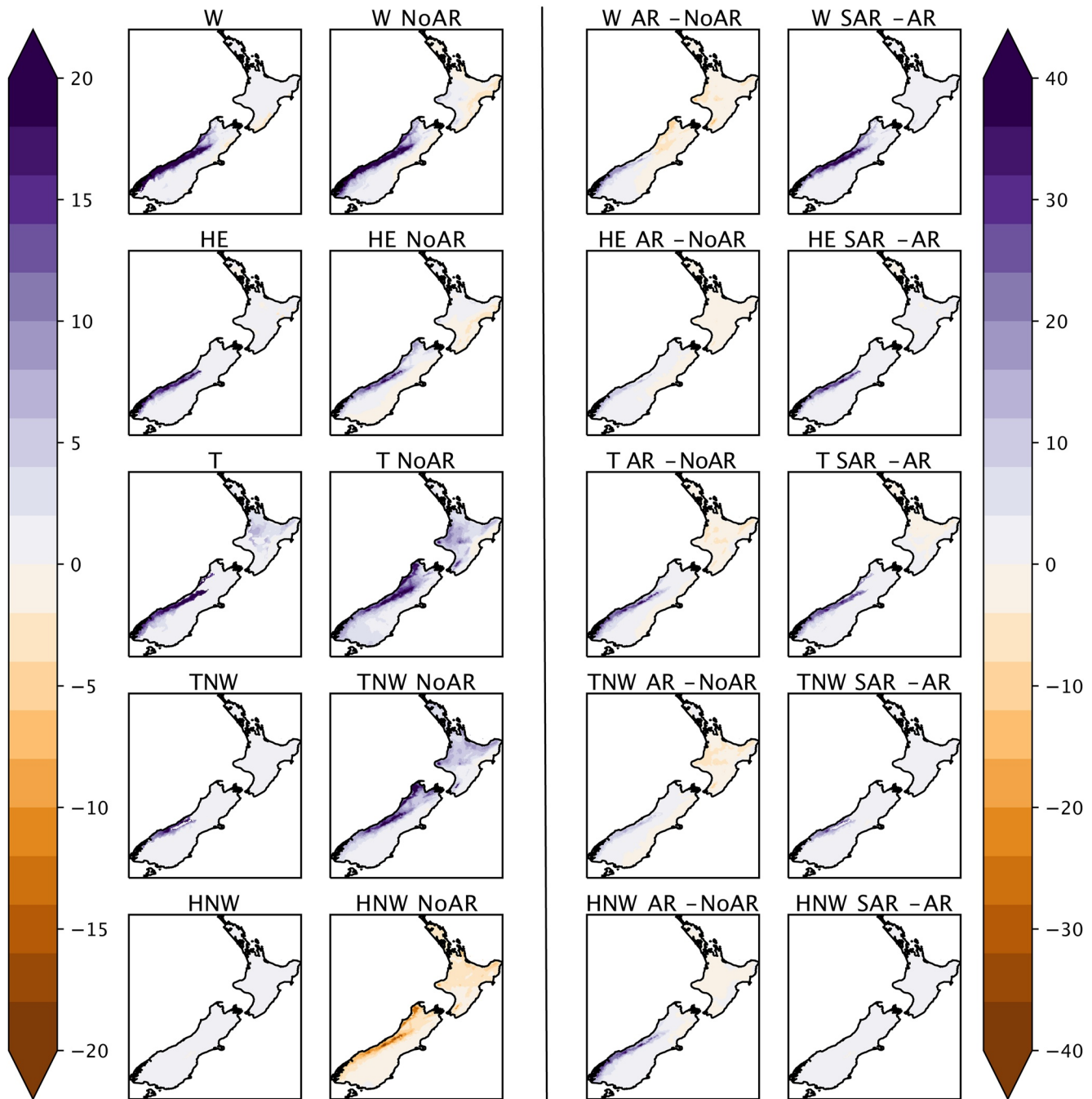


Figure 6. Daily precipitation anomalies (mm) associated with weather types (WTs) when associated and not associated with atmospheric rivers (ARs), West Coast region of Aotearoa New Zealand. Composite precipitation anomalies (mm) during the five most favorable WTs (all days considered: first column) and during their occurrences not associated with ARs (second column), differences between NoAR days and moderate AR days (third column), and differences between strong AR days and moderate AR days (fourth column). For the two first columns (left-hand colorbar), only significant anomalies against the climatology according to one-tailed *t*-tests modified by Welch (95% level) are displayed. For the third and fourth columns (right-hand colorbar), only significant differences according to two-tailed *t*-tests modified by Welch (95% level) are displayed. ERA5 redefinition of WTs is used.

4.2. Precipitation Extremes

Because of the strong spatial contrasts in precipitation amounts, and their variability, across ANZ, considering the mere amplitude of anomalies as done in Figure 6 is not convenient to assess to which extent WTs and ARs contribute (jointly or separately) to precipitation extremes. Hence, with Figures 7 and 8, we explore to which

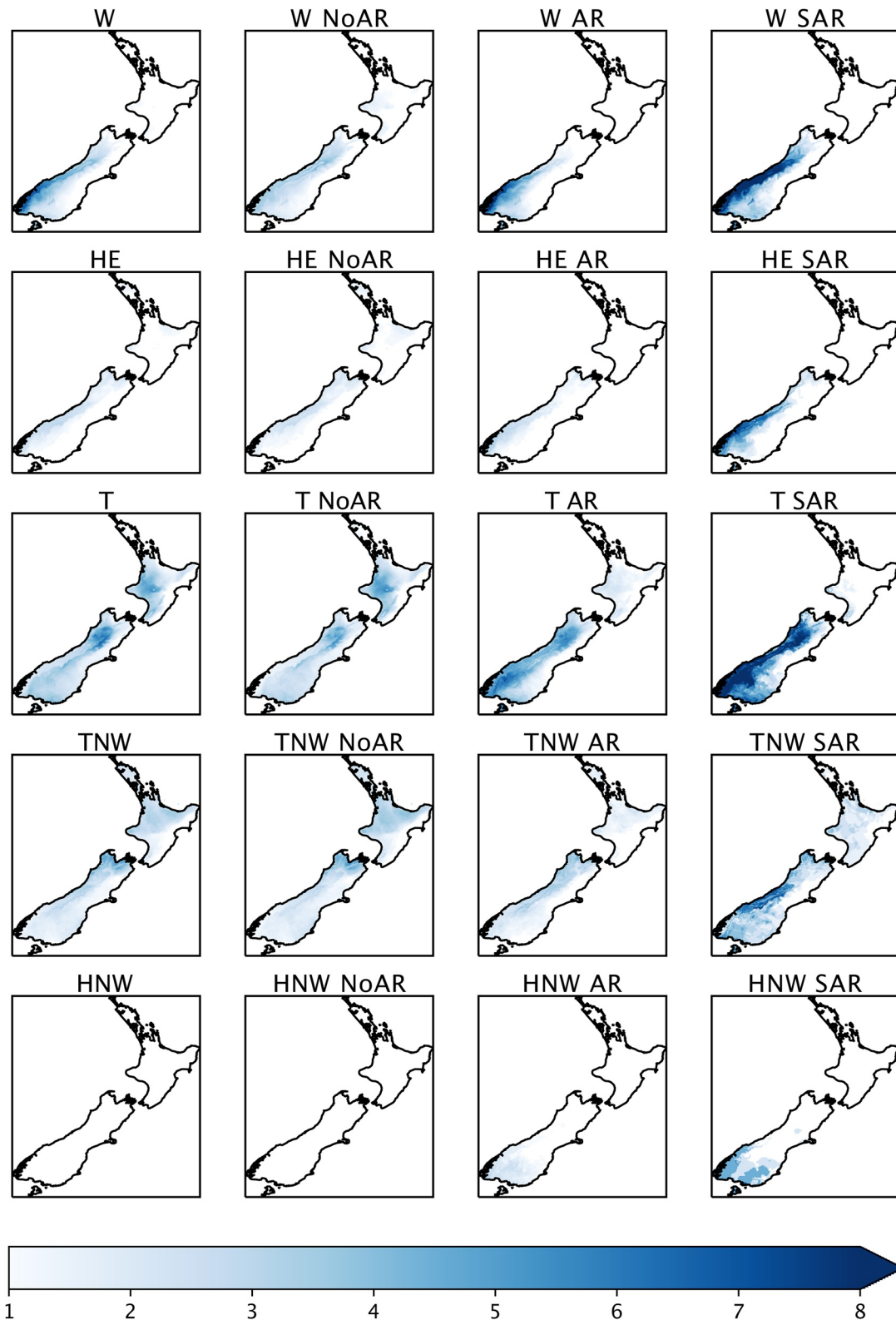


Figure 7. Probability ratios for daily precipitation anomalies exceeding the 95th percentile for the five most favorable weather types (WTs), for the West Coast region of Aotearoa New Zealand, and for: first column, all days of the WT (against all days of all other WT), second column: NoAR days (against all days of all other WT), third column: moderate atmospheric river (AR) (against NoAR days of the same WT) and fourth column: strong AR days (against NoAR AR days of the same WT). Probability ratios less than 1 are shaded white. ERA5 definition of WT is used.

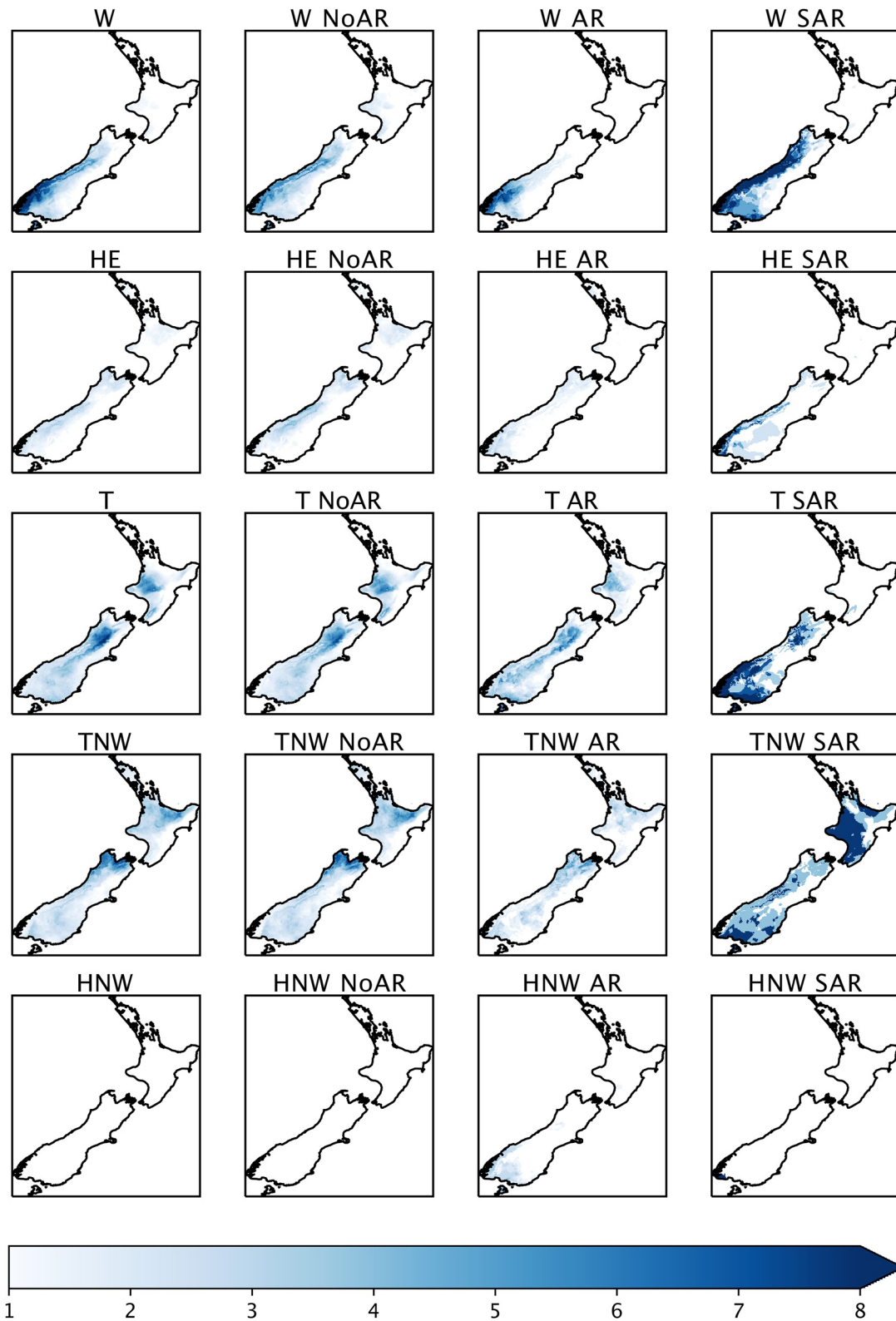


Figure 8. Probability ratios for daily precipitation anomalies exceeding the 99th percentile for the five most favorable weather types, for the West Coast region of Aotearoa New Zealand. All analyses and probability ratios are calculated and represented as in Figure 7.

extent ARs, and their most favorable WT, are over-represented in daily precipitation extreme occurrences, and could therefore be considered as one of their main drivers. For each occurrence of a favorable WT (either associated or not with an AR event) in the West Coast of the South Island, we calculate the probability ratio to exceed the 95th and 99th percentiles of daily precipitation anomalies, between contrasted groups of days. First, these ratios are calculated for all days ascribed to one of the most AR-favorable WTs, against all other WTs; the same is done only for NoAR days within the same WTs. This makes it possible to assess the influence of a given WT on extreme occurrence, when including or excluding AR days. Next, during each of these AR-favorable WTs, the probability ratios are calculated between NoAR and moderate AR days on the one hand, and NoAR and strong AR days on the other hand. This second step further explores within-type diversity as explained by AR occurrence, and their influence on precipitation extremes. Figure 7 shows results for the 95th percentile, and Figure 8 for the 99th percentile, for the West Coast region. These analyses, duplicated for all seven landfalling locations around ANZ (see Figure 1b), show strong regional-dependency. In order to focus on more inhabited regions and also to illustrate the diversity and regional dependency of our results, analyses for the South Coast and Northland regions of ANZ are given in Figures S4–S7 in Supporting Information S1.

When considering their total occurrences, these WTs all tend to promote daily extremes in the West Coast region, except type HNW (identified as near-normal on average there: Figure 6). Type HE shows the weakest over-representation of precipitation extremes, and was also previously identified as conducive to anomalously wet conditions on the West Coast, but with magnitudes weaker than the remaining three types. The probability of a daily precipitation extreme moderately decreases for the NoAR category (except for HNW; Figures 7 and 8). In sharp contrast, daily precipitation extremes along the West Coast are much more frequent during moderate, and even more clearly, strong ARs. Daily precipitation extremes there are much favored by the co-occurrence of these selected WTs and ARs: for types W, T and TNW and for the 95th threshold (Figure 7), their probability ratios often exceed 4 and even 7–8 for types W and T. Type W also supports a marked increase in 99th percentile extreme occurrence, west of the main mountain range of the Southern Alps. Probability ratios there for 99th percentile extremes are smaller for types HE and TNW; types T and HE more particularly favor extremes for the south-westernmost parts of ANZ, but its influence decrease toward the North. Type TNW, on the other side, is also associated with enhanced extreme occurrence over the North Island of ANZ, that is, far out of the West Coast, in regions showing more exposure to northerly anomalies. This is consistent with the northwesterly circulation anomalies associated with this type near ANZ (Pohl et al., 2023). Even during ARs or strong ARs, type HNW does not yield increased extreme occurrence. This type, while often co-occurring with ARs (Figure 5), is therefore mostly associated with quite weak to moderate precipitation intensities.

These AR-favorable WTs in the West are generally conducive to much drier conditions along the eastern coast of the South Island, corresponding to the flatter coastal regions of Canterbury and Otago, and are only weakly associated with increased probabilities of daily precipitation extremes there, even during strong ARs (Figure 6). Even strong ARs landfalling on the West rarely lead to exceed the highest percentiles of daily anomalies on the leeward side of the main divide (Figures 7 and 8). Intrusions to the East are more frequent in the North Island and in the southern parts of the South Island, where the elevation of the mountains gradually decreases.

In the Supporting Information S1, we further show that ARs and their most favorable WTs often cause precipitation extremes in the northern parts of the country (where ARs often correspond to poleward moisture transport from the subtropical latitudes). In the southern regions, ARs are much more related to mid-latitude dynamics, and their efficiency to produce large precipitation amounts, including extremes, appears much reduced. A noticeable exception is the southwestern tip of ANZ, because of the stronger topographic lifting and the exposure facing the dominant westerly winds.

Overall, this section confirmed that AR events are responsible for heavy precipitation amounts in ANZ, and are likely to strongly modulate the influence of the 12 WTs of K2K on precipitation variability and amounts. Intense to extreme daily precipitation anomalies tend also to occur preferentially during ARs, with their probability being typically multiplied by 4–5 and up to 8–10 as compared to NoAR days occurring during the same WTs.

5. AR and WT Inter-Relationships

It seems reasonable to expect AR properties (Table 2) to be partly driven by the location and intensities of synoptic ACAs (as is the case for Europe, the North Pacific and East Antarctica: see Eiras-Barca et al., 2018;

Fish et al., 2019; Pohl et al., 2021c, respectively). Here, ACAs are themselves discriminated by the 12 discrete synoptic WTs and their associated quantitative descriptors (Table 1). In this section, we assess how these two families of atmospheric circulations are interrelated, over and near ANZ.

5.1. Synoptic Control on AR Properties

Figure 9 shows the statistical distribution of all AR properties, presented here as violin plots, for each WT and for the West Coast region. The same analyses for the two most remote grid-points are shown in Figures S8 and S9 in Supporting Information S1. Analysis of Fisher's test shown in Figure 9 for all quantitative metrics (thus excluding AR directions) suggests that synoptic conditions, monitored through the 12 WTs, strongly and significantly influence AR characteristics, with estimated statistical significance exceeding the 99.99% ($p < 10^{-4}$). These statistics are likely biased by the large sample sizes.

Figure 9 reveals that both zonal and meridional components of IVT, for these AR events reaching the West Coast region, strongly differ from one WT to another. Although the zonal component is shifted toward positive values (denoting a westerly component that was expected at these latitudes), some WTs (namely, TNW, HSE, HE, and particularly NE: Figure 9) favor more balanced or more variable signs suggesting recurrent easterly advections. The meridional component similarly shows a shift toward negative values indicative of moisture transport from the lower latitudes, but some WTs (SW, HNW, HW) also correspond to ARs with a marked southerly component. These results are true when all timesteps of the AR lifecycles are considered, but also hold for the only maximum of moisture transport (with generally stronger values). Overall, when combined, these results show that the WTs have a strong influence on AR directions (Figure 9). This conclusion is also true for other regions of ANZ (Figures S8 and S9 in Supporting Information S1), although the filtering used here to select ARs coming only from the sea may also strongly decrease the statistical spread of AR directions, depending on the geometry of the coastline (Figure 5; Figures S8 and S9 in Supporting Information S1).

Finally, WTs also modulate AR durations and their time-integrated total IVT. While types HNW and HW tend to coincide with the less persistent ARs (as shown by a median duration of just 6 hr, i.e., the AR detection timestep), types HSE, W, HE and NE are associated with much longer AR events, as indicated both by their median duration (18 hr, i.e., 3 detection timesteps) and largest values (reaching or exceeding 4 days, i.e., 96 hr). Time-integrated total IVT (and their WT-dependency) are very consistent with the duration, the longer events logically leading to larger moisture advections. These duration statistics of AR events embedded in WT sequences appear quite disconnected from the typical persistence of the WT sequences themselves, as assessed by K2K (his Figure 4): the most persistent WTs are not those conducive to the most persistent ARs. The latter are also 2 to 3 times shorter, suggesting that ARs preferentially develop within WTs in a vast majority of cases, rather than during the transition from one WT to another. Because of their weak persistence, AR events associated with more than one WT are rare, especially when WTs are defined at the daily timestep as done for this work.

The results discussed above generally hold for all grid-points shown in Figure 1b and used for AR detection, in spite of a tendency for more persistent AR sequences over the northern parts of ANZ. Despite major differences in sample sizes (in terms of AR count and their association with synchronous WTs: Figures 4 and 5), WT influence on AR properties appears strongly consistent from one region of ANZ to another (not shown).

5.2. Synoptic Differences Between AR and NoAR Days

In addition to the relationship between WT and AR occurrence, do ARs influence WT synoptic patterns in return, and/or develop within synoptic patterns that may differ from the mean view of the WT, as obtained when merging all days? This hypothesis, if verified, (a) would be consistent with the strong within-type variability suggested in Section 4 and based on daily precipitation fields, (b) would be in line with the results of Eiras-Barca et al. (2018) over the northern mid-latitudes, or Pohl et al. (2021c) over the southern high latitudes. It is therefore tested below.

Figure 10 shows changes in the regional-scale circulation (geopotential height and horizontal wind anomalies at 700 hPa) during the five WTs most favorable to ARs in the West Coast, and separates NoAR days from moderate and strong AR events. Figure 11 similarly presents the 1000 hPa specific humidity and moisture flux anomalies at 1000 hPa, these fields being of major importance for IVT and, therefore, for AR influence in ANZ. Both definitions of the WTs are used in both figures, because they lead to slightly different results (both in terms of

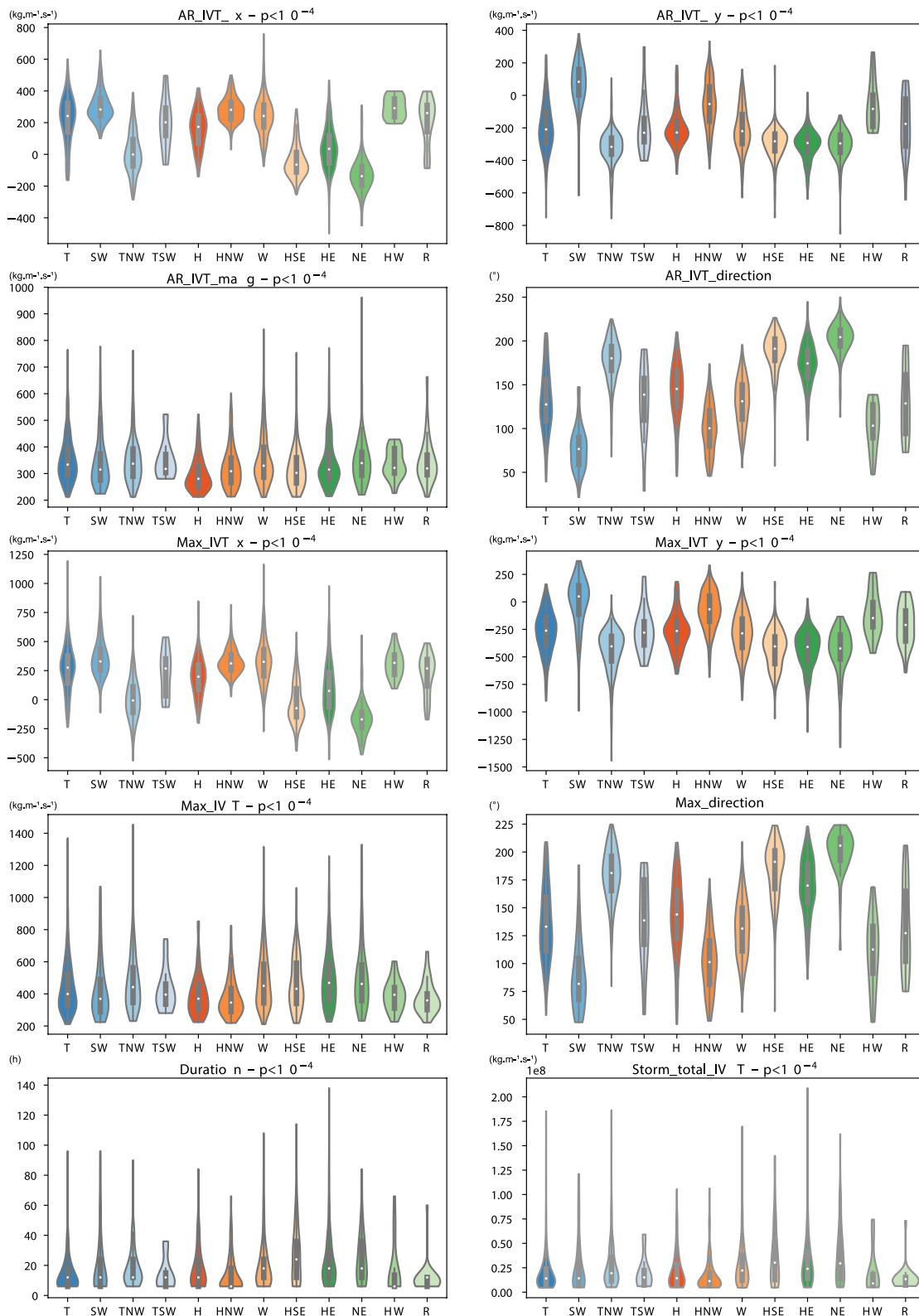


Figure 9. Modulation of atmospheric river (AR) properties by the weather types (WTs), West Coast region of Aotearoa New Zealand. Inner boxes: from first to third quartiles (50% of the samples) with median value given by white circles. Whiskers show the range of the distributions, and violin plots represent smoothed observation densities. For quantitative values (all except IVT directions), labels indicate the estimated significance according to analyses of variance. WT are colored as in Figure 5. The number of AR days N used in these analyses is given in Figure 4c ($N = 5,909$). ERA5 definition of WT is used.

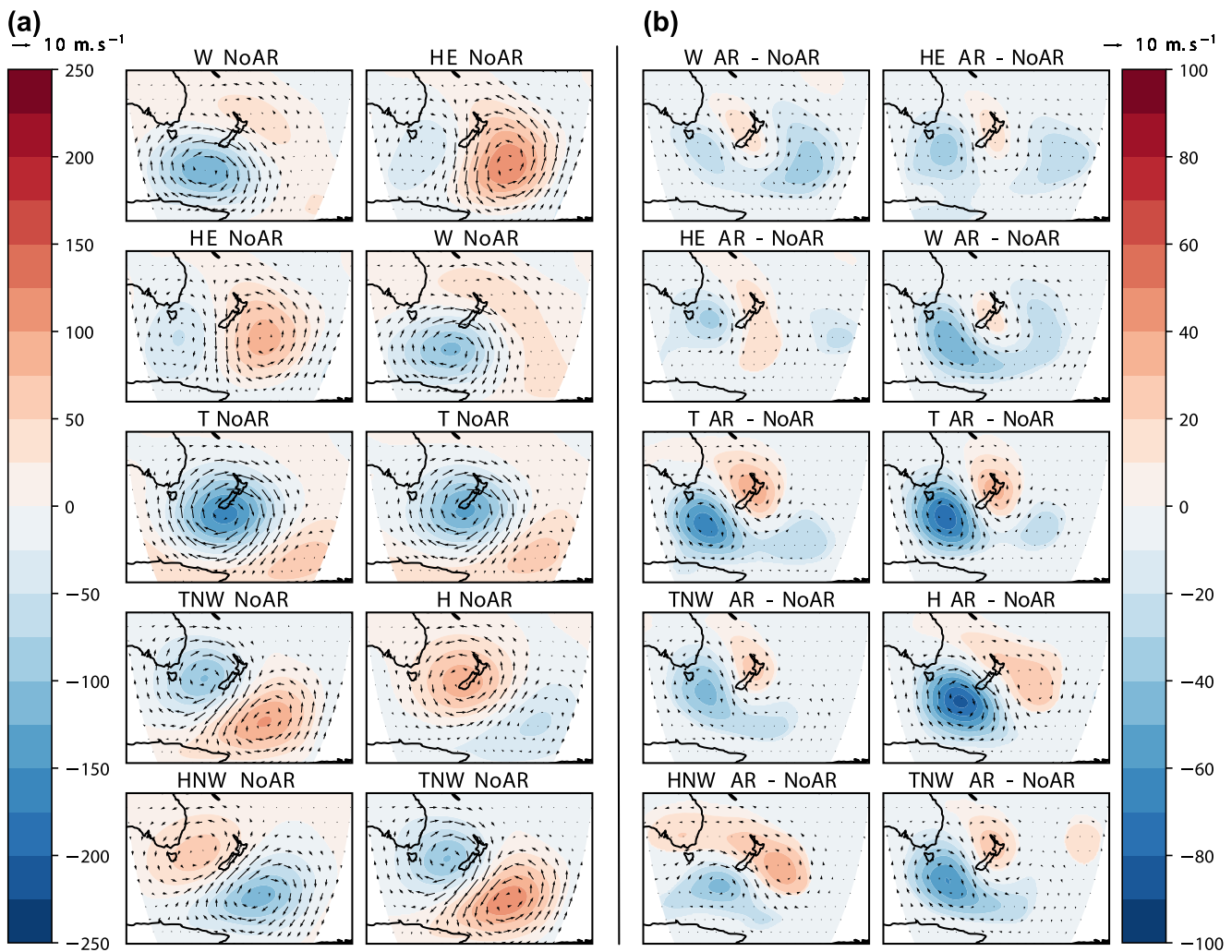


Figure 10. Differences in synoptic conditions between weather types (WTs) associated and not associated with atmospheric rivers (ARs), West Coast region of Aotearoa New Zealand. (a) Composite mean geopotential height anomalies at 700 hPa (colors: m) and 700 hPa horizontal wind anomalies (vectors: m s^{-1}) anomalies during the five most favorable WTs, and for the ERA5 redefinition of WTs (first column), and the original NCEP/NCAR definition of the WTs (second column). Only significant anomalies according to one-tailed t -tests modified by Welch (95% level) are displayed. (b) Difference between AR and NoAR days for the same WTs, and for the ERA5 redefinition of WTs (first column), and the original NCEP/NCAR definition of the WTs (second column). Only significant differences according to two-tailed t -tests modified by Welch (95% level) are displayed.

preferential associations between WTs and ARs, Figure 5, and within-type differences): please refer to Pohl et al. (2021b, 2023) for more details. Figures S10 and S11 in Supporting Information S1 generalizes the results of Figure 10 results for the South Coast and Northland regions of ANZ, respectively, and Figures S12 and S13 in Supporting Information S1 similarly extend the results of Figure 11.

Daily geopotential and circulation anomalies associated with these WTs when not co-occurring with ARs are similar to the average pattern of these types (Figures 10 and 2). They are also generally quite consistent for both WT definitions (Figure 10a), even though ACAs (and more particularly the negative ones, indicative of atmospheric troughs) tend to reach larger intensities using the newer ERA5 distribution. This is probably due to the more detailed and accurate resolution of the ridges and troughs in ERA5, in line with its finer grids. These WTs favor moisture transport toward the West Coast of the South Island, either from the west or northwest (for types W, HE, and TNW) or southwest (T and HNW).

Within-type differences between NoAR and AR days are weaker (half the magnitude) than the mean departures from the mean annual cycles during the overall occurrences of this type (Figure 10b). This indicates that, even during AR days, the concomitant WTs are still well characterized by their main synoptic-scale specific patterns.

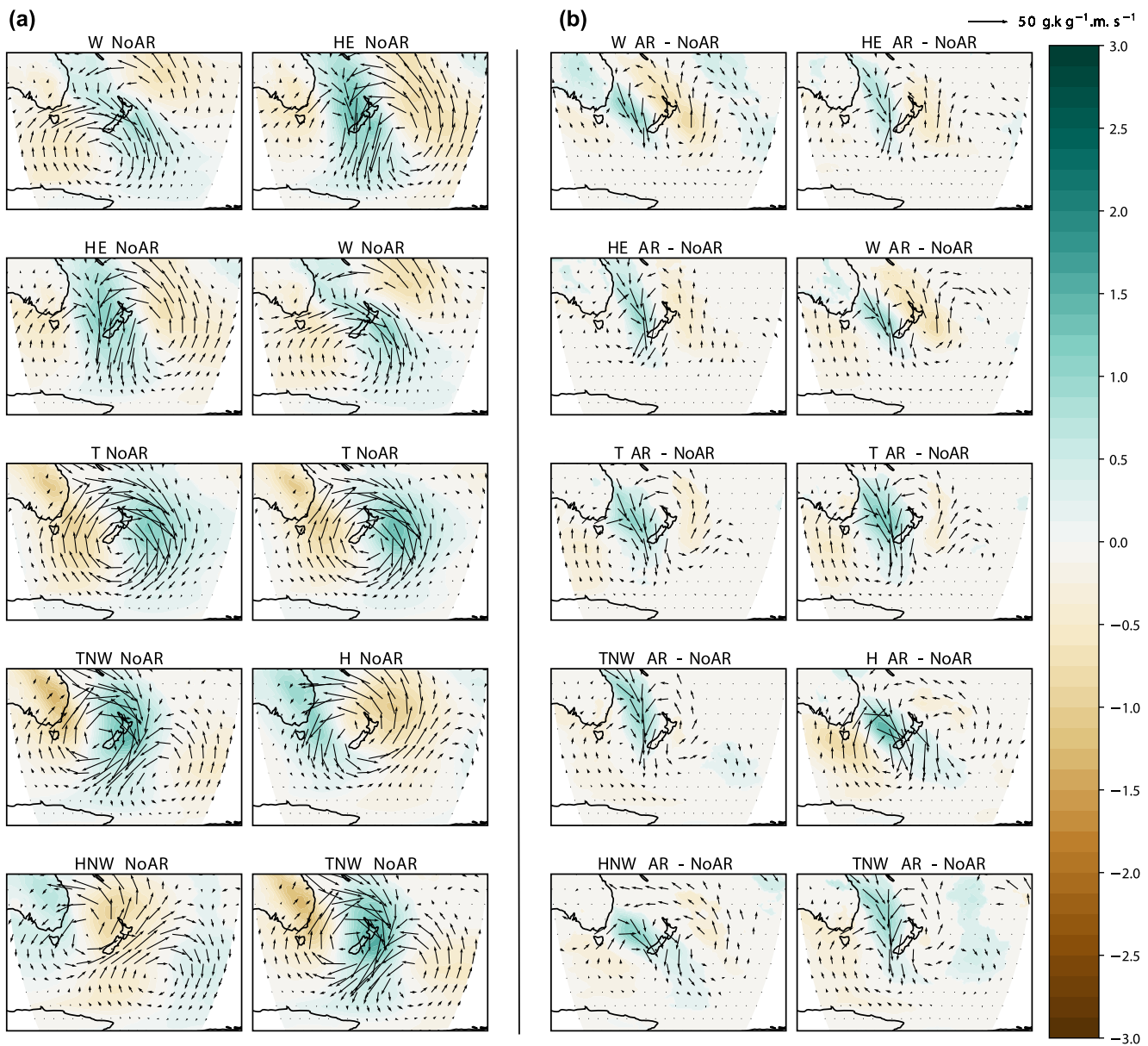


Figure 11. As Figure 10 but for specific humidity at 1,000 hPa (colors: g kg^{-1}) and 1,000 hPa horizontal moisture fluxes (vectors: $\text{g kg}^{-1} \text{ m s}^{-1}$).

Such within-type differences between NoAR and AR days are remarkably similar across the types, and do not appear to be directly related to the mean anomaly patterns of the types. For all WTs, they consist in a dipole of geopotential height, with positive differences northeast of ANZ, and negative ones west (and, for some types, south) of it. This dipole is thus associated with a stronger geostrophic northwesterly component of the winds, which favors moisture transport from the lower latitudes (Tasman and/or Coral Seas) toward the West Coast of the South Island, perpendicularly to the main topographic barrier of the Alps. Albeit their weaker magnitudes, these differences are very consistent with the AR patterns landfalling there, as discussed in the literature (Cullen et al., 2019; Kingston et al., 2016, 2022; Little et al., 2019; Prince et al., 2021a; Reid et al., 2021; Shu et al., 2021). Within-type differences are also much larger according to the original NCEP/NCAR definition of the WTs (Figure 10b), especially the negative geopotential height differences located west or southwest of ANZ. Figures S10 and S11 in Supporting Information S1 confirm these conclusions for other parts of ANZ, although the location and orientation of the geopotential dipole changes, so that the resulting fluxes reach the landfalling region with stronger westerly/southwesterly (for the South Coast region: Figure S10 in Supporting

Information S1) or northerly/northwesterly components (for the Northland peninsula: Figure S11 in Supporting Information S1).

In contrast with the marked differentiation between NoAR and moderate AR days, differences between strong and moderate ARs seem much noisier and less coherent, spatially and physically (not shown). This suggests that the intensities and location of the main ACAs could have limited control on the strength of landfalling ARs, as inferred by their IVT. Thus, the strength of the ARs could possibly be more related to the moisture content of the air mass, than stronger synoptic ACAs. By analyzing anomalies of specific humidity and moisture fluxes around ANZ, Figure 11 aims at exploring this issue. Here, lower-layer moisture fluxes are shown, together with anomalies of specific humidity at 1,000 hPa, during overall WT occurrences. Next, we analyze the within-type diversity, by calculating the differences between NoAR and AR days. Figures S12 and S13 in Supporting Information S1 complement this figure for the South Coast and Northland regions.

These results (Figure 11a) generally confirm previous work concluding that southerly anomalies advect dry air toward ANZ, northerly fluxes having an opposite effect (e.g., Pohl et al., 2021c, 2023). Furthermore, they point out that the air mass contains significantly more humidity during AR days (Figure 11b). These results are coherent with Figure 10, the stronger northwesterly component of the lower-layer circulation favoring moisture export from the lower latitudes. These conclusions can be extended to strong ARs, which significantly differentiate from regular ARs in terms of air moisture but not significantly in terms of geopotential anomaly patterns (not shown).

However, Figures S12 and S13 in Supporting Information S1 (which respectively generalize these analyses for the South Coast and Northland regions of ANZ) reveal strong regional dependency of the moisture sources, which raise important questions related to the physical nature of the mechanisms associated with moisture transport. These figures show that moisture transport reaching the southernmost parts of the country do not seem to originate from the lower latitudes, but are embedded in the extratropical westerly circulation. The situation is quite different in the northern regions, where the connection with the subtropical Coral and Tasman Seas is more evident. This could question whether the strong moisture transport landfalling in southern ANZ do correspond to ARs (following e.g., the definition of Ralph et al., 2018), or transient enhancement of the mid-latitude westerlies, implying thus stronger zonal moisture transport but limited meridional export from the lower latitudes.

Overall, our results suggest that synoptic conditions have strong importance for AR development and for shaping their location and angle, while corresponding IVT seems to be influenced by the available moisture content in the subtropical latitudes that can next be advected southwards once the AR is formed. These results are verified for the northern regions of ANZ, they still hold for the West Coast of the South Island, but air humidity from the subtropics seems of little importance for the southernmost parts of the country (Figure S13 in Supporting Information S1). The different moisture sources, from higher latitudes, that could affect this part of the country, corroborate the results of Bennet and Kingston (2022) on the spatial patterns of IVT in ANZ, and are also coherent with Reid et al. (2022) who obtained similar results for Australia. More detailed assessment of moisture sources is now needed, for example, through Lagrangian approaches, but this is not our scope here.

5.3. Interactions Between AR Properties and Synoptic Configurations

Section 5.1 discussed how synoptic configurations, as materialized by the 12 WTs, modify AR features. Section 5.2 further established that synoptic configurations themselves differ depending on the presence, absence, and for some cases, strength of the AR events. Here, we attempt to reconcile these views, and analyze these interactions in a unified way. Figures 12 and 13 show how AR attributes (as summarized in Table 2) relate to the synoptic descriptors of ACAs (as summarized in Table 1). These analyses are done for each day ascribed to the five more favorable types promoting the largest numbers of ARs reaching the West Coast region. Very similar results are obtained for other landfalling regions in other parts of ANZ, with their respective AR-favorable WTs (not shown).

Whatever the definition of WTs, Figures 12 and 13 indicate that the intensity of atmospheric ridges is significantly related to changes in AR properties. This is especially true for types TNW, W, and HE. The T type has no positive ACA: it mostly relates to changes in AR characteristics through the latitude, and to a lesser extent, the intensity, of its main atmospheric trough. In spite of the statistical significance of some associations between within-type diversity and AR properties, the common variance between corresponding couples of descriptors remains low. This may be due (a) to the large sample size (exceeding 1,800 days for the chosen grid-point

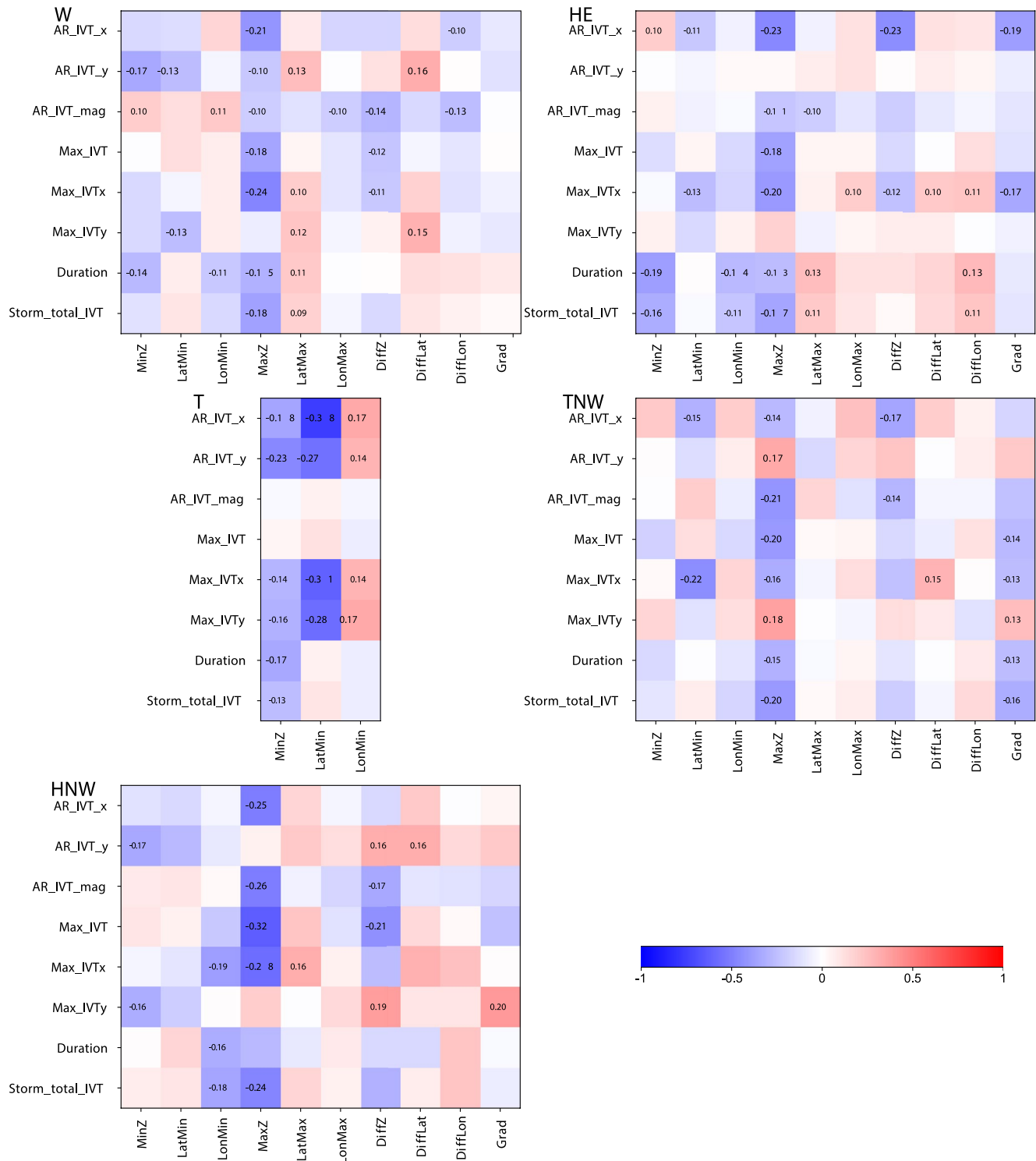


Figure 12. Daily correlations between KT descriptors and atmospheric river features for the 5 most favorable KTs according to ERA5 definition of weather types (WTs) for the West Coast region of Aotearoa New Zealand, and for the ERA5 redefinition of WTs. Correlations not significant at 95% omitted, correlations above the 99% threshold in bold.

representative of the West Coast region: Figure 4), and/or (b) to the fact that we are considering here residual variability, the main changes being likely associated with differences between WTs (Section 5.1). Nevertheless, this still suggests that, under a given synoptic context, AR diversity, from 1 day or event to another, cannot be interpreted as simple linear functions of the location and intensities of ACAs. These general conclusions and

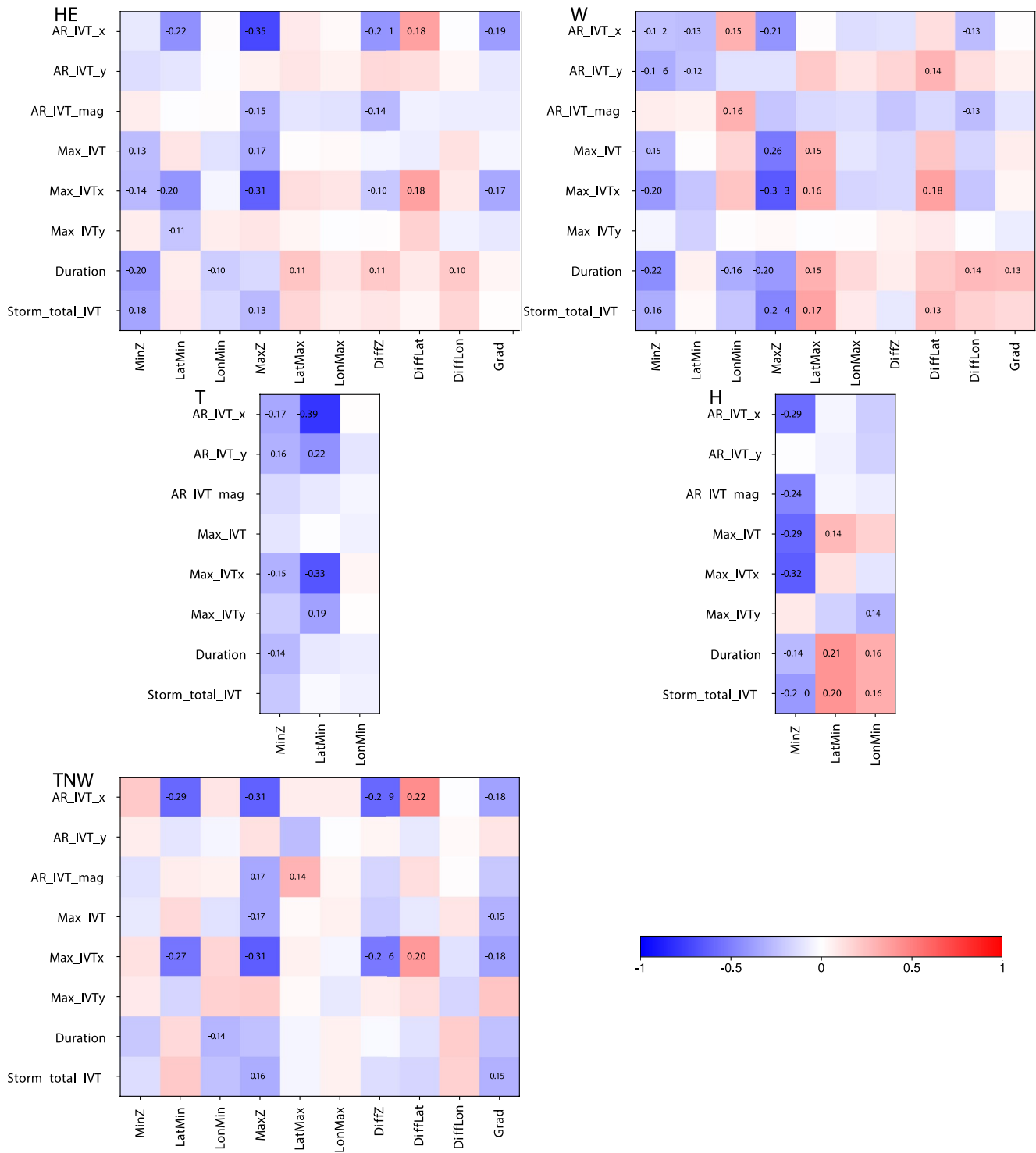


Figure 13. As Figure 12 but for the original NCEP/NCAR definition of the weather types.

results, including a significant but still moderate role of the intensity of atmospheric ridges, are also verified for all other regions of ANZ (not shown).

How within-type diversity could relate, physically, to changes in AR properties, cannot be assessed based on correlation analyses. The negative correlation between ridge intensities and moisture transport may also seem counter-intuitive, strong ridges or blockings being mentioned in the literature as a favorable condition for moisture

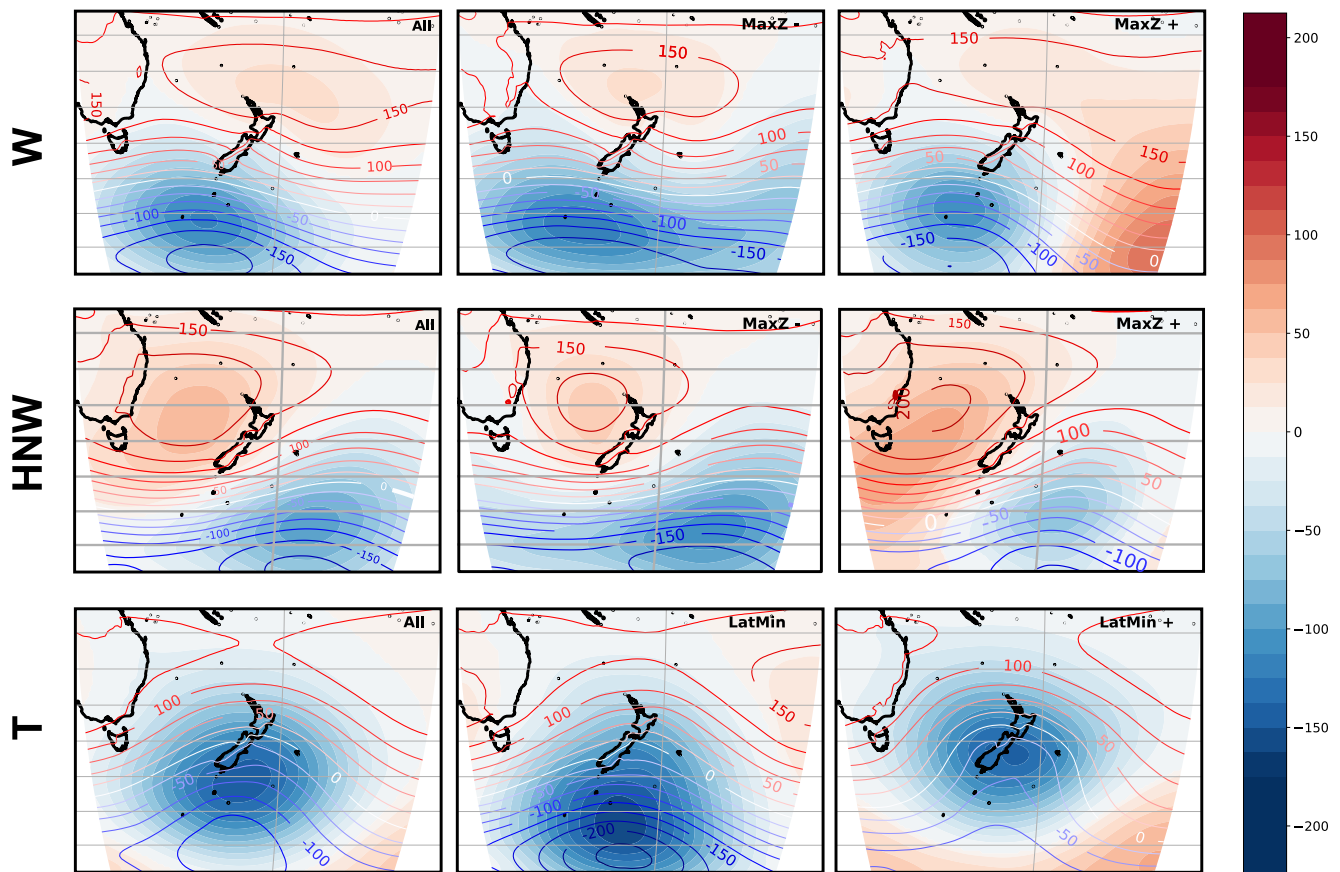


Figure 14. Composite mean Z1000 fields associated with the opposite phases of weather type (WT) descriptors for WTs W, TNW, and T controlling atmospheric river differences in grid-point #6 (West Coast of the South Island). The left-hand column shows the composite mean anomaly pattern of Z1000 raw fields (contours) and corresponding anomalies (colors) during all days ascribed to the corresponding WTs. The two remaining columns show the sub-samples formed by the opposite phases of the WT descriptor labeled in the figure. Opposite phases of each descriptor of each WT are extracted using their 20th and 80th percentiles. In all maps, only significant anomalies according to one-tailed *t*-tests modified by Welch (95% level) are displayed.

transport channeling and, thus, AR development (Pohl et al., 2021a). Hence, Figure 14 shows composites of the opposite phases of the synoptic descriptors found in Figures 12 and 13 to influence AR properties. The composite approach used here (based on the 20th and 80th percentiles of each descriptor), discussed in P21, does not assume that relationships are linear, as do the correlation analyses of Figures 12 and 13. Qualitatively similar results could be obtained with other percentile values (not shown).

The W type is formed by a strong negative ACA southwest of ANZ and a weaker positive one north it, that channel westerly winds toward the country (Figure 14), hence its strong contribution to AR occurrences for parts of ANZ (Figure 5). It is the positive ACA that mostly acts to modify AR properties, with larger ridge intensities corresponding to reduced moisture transport (Figures 12 and 13). Strongest ridges actually correspond to a Z1000 pattern that sensibly differs from the canonical view of that WT, with an alternation of atmospheric waves in the mid-latitudes that is associated with stronger sinuosities of the westerlies. This could correspond to generally weakened winds, hence the decreased moisture transport. Similar results are obtained with type TNW (not shown) or HNW (Figure 14): particularly strong ridges clearly increase the transient wave component of mid-latitude circulation, as compared to the weaker ridge occurrences associated with this type. As a result, corresponding AR events exhibit a weaker zonal moisture transport.

The T type is the most favorable one for AR development for many parts of ANZ (Figure 5). It shows a single negative ACA consisting in a trough (hence its name) located near or just south of ANZ. The negative correlations between IVT on the one side, and the intensity and latitude of the troughs on the other side, imply that stronger troughs (larger negative values of geopotential height anomalies), and/or southernmost locations, both favor increased moisture advections linked to ARs. Indeed, both types of configurations increase westerly winds north

of the trough (Figure 14), leading to stronger atmospheric fluxes meeting the coasts and mountains of ANZ. Similar mechanisms also prevail for the troughs associated with types W, TNW, and HE, albeit their weaker correlations (Figures 12 and 13).

This section pointed out how synoptic ACAs, by modulating the westerly wind speeds, can modify AR-associated IVT toward the West Coast of ANZ. These relationships remain quite weak, despite their statistical significance. A possible reason is that our analyses are only based on atmospheric dynamics, hence the need to consider air humidity and to identify moisture sources in future work (in agreement with Figure 11).

6. Discussion and Conclusion

In this work we analyze relationships between the 12 WTs of Kidson (2000), defined over the ANZ sector, and ARs, as detected by the Guan and Waliser (2019) algorithm participating to the ARTMIP-Tier2 inter-comparison exercise (Marquardt Collow et al., 2022), that make landfall in different parts of ANZ. Focus is given on inter-type variability, and how differences in the weather patterns around ANZ act to modify AR properties (angle, water vapor transport, ...), as well as within-type diversity, and how it relates to AR variability. To that end, two series of descriptors are used: they monitor, on the one hand, the intensity and location of main ACAs associated with the WTs, and on the other hand, the angle, duration and moisture transport associated with the ARs. Analyzing jointly the co-occurrences of WTs, ARs, and their respective descriptors, allowed us to explore how they are interrelated, thereby complementing the more usual analyses of AR probability depending on the synoptic context, or the relative contribution of each WT to overall AR occurrences. The relative importance of inter-type versus within-type diversity is also addressed from a precipitation point of view, by assessing the combined and separate influence of WTs and ARs on daily amounts across ANZ. The case of precipitation extremes is considered, ARs being recurrently identified as a key driver of such precipitation excesses.

Our main results can be summarized as follows.

- While ARs make landfall, on average, about 12% of the time in (any) part of the coastlines of ANZ, they contribute to 62% of the occurrences of moisture transport exceeding $250 \text{ kg m}^{-1} \text{ s}^{-1}$ (a threshold often used in the AR community, e.g., Ralph et al., 2019), and nearly 95% of the occurrences with an IVT above $500 \text{ kg m}^{-1} \text{ s}^{-1}$. This confirms (a) the predominant importance of ARs on moisture transport toward ANZ, and (b) that detecting ARs is an appropriate way to detect on a vast majority of the very strong to extreme moisture fluxes landfalling in ANZ.
- AR occurrences display clear preferential associations with a few WTs, and these associations are strongly region-dependent across ANZ. The most favorable WTs are, quite logically, those that act to direct moisture fluxes toward the country. However, a more meaningful result is that, for a given region, the most favorable WT is responsible, at most, for only a third of overall AR events. Generally, three or four WTs can be identified as the main drivers of ARs, for a given region. These WTs strongly differ from one part of ANZ to another, the most recurrent favorable types being those that promote increased westerly, or a marked north-westerly component, to the regional atmospheric circulation.
- Within-type and inter-event variability and diversity is large, both for ARs and WTs. Some AR attributes are strongly modulated by WTs. This is especially the case for their angle, but their persistence also differs between WTs.
- When co-occurring with AR events, the WTs tend in return to show changes in the location of their main ACAs, that act to deviate the winds toward ANZ. ACAs do not appear to be significantly more intense during the strongest ARs, that is, those associated with the largest moisture transport. However, the air mass is significantly more moist during the latter events, especially north of ANZ. While AR occurrence, location and angle are favored and largely driven by synoptic-scale variability, vapor transport appears more tightly related to lower-layer specific humidity (especially for the northern regions of ANZ, connected with subtropical regions during major AR events). For the southern regions, key features involve the velocity of mid-latitude westerly winds, while links with the subtropical latitudes are weaker. Whether such increase in the westerlies correspond to ARs is an issue that we further discuss below.
- Within-type variability has also major consequences for precipitation variability, and for the occurrence of daily extremes. The composite mean anomaly patterns of precipitation conceal major changes between NoAR and AR days. Strong AR events (in terms of moisture transport) also differentiate from moderate events. The same WTs only yield weak anomalies when not co-occurring with ARs, or even, in some cases, anomalies

of opposite sign (i.e., drier than normal). AR influence is particularly strong for wet extremes: depending on the regions, the probability for daily precipitation extremes can be multiplied by 8–10, between AR days and NoAR days ascribed to the same WT.

This study illustrates how WTs can drive and/or modify AR development and their associated attributes. The reverse relationship remains still unclear to date. Another major aspect to consider could then be to assess to what extent ARs influence WTs in return, that is, modify the strength and/or location of their main ACAs. Differentiated evolutions of ACAs would be consistent with larger latent heat release during ARs, increasing cyclogenesis through differential diabatic heating profiles (Madonna et al., 2014; Terpstra et al., 2021; Woollings et al., 2018). A more detailed analysis of the life cycle of these ACAs could be performed, for instance using analogs, in order to determine whether they evolve differently under AR and NoAR conditions.

In spite of ARs' predominant importance for moisture transport in the region, the present work also raised the question of their definition and detection criteria, and how to differentiate ARs from other types of moisture transport in the troposphere. ARs are defined in the American Meteorological Society Glossary of Meteorology as “a long, narrow, and transient corridor of strong horizontal water vapor transport that is typically associated with a low-level jet stream ahead of the cold front of an extratropical cyclone.” The relevance of this definition has already been extensively discussed by Ralph et al. (2018). Here, we show that detected ARs, while responsible for a vast majority of strong to extreme moisture transport toward this region, are not restricted to being associated with extratropical cyclones. In ANZ, landfalling ARs can be driven by other synoptic scale features (including tropical cyclones: e.g., Prince et al., 2021a). Similarly, ARs in the polar regions (Gorodetskaya et al., 2014), also discussed as narrow long bands of enhanced moisture fluxes originating from the mid-latitudes and subtropics (Wille et al., 2022), were also found to develop when a ridging or blocking highs located further east act to channel the geostrophic flow toward the higher latitudes (Pohl et al., 2021a), thereby transporting heat and moisture poleward. In this regard, the association between ARs and extratropical cyclones, as mentioned in the glossary, may appear as slightly too restrictive to encompass the diversity of synoptic configurations likely to lead to AR development worldwide.

Thus, while the majority of ANZ ARs may be associated with an extratropical cyclone there is certainly a diversity of synoptic configurations that give rise to extreme moisture fluxes, detectable as ARs in the region of ANZ.

The case study of ANZ can also be used to discuss the detection criteria for ARs, and especially the role of meridional transport of moisture and heat. ARs landfalling in the northern parts of ANZ are in very good agreement with the typical image one can have of ARs landfalling in the southern mid-latitudes (Bennet & Kingston, 2022; Kingston et al., 2022; Prince et al., 2021a), that is, a connection linking the (sub)tropical latitude to the extra-tropics, probable moisture sources located over the Coral and Tasman Seas east of Australia, and larger occurrence during the austral summer season. By contrast, in the southern regions of ANZ, placed under the direct influence of the dominant mid-latitude westerly winds, detected AR events are more zonal, and show limited connection with the lower latitudes—a matter also discussed more generally by Guo et al. (2020) or Gimeno et al. (2021). Potential moisture sources for ARs landfalling in the southernmost parts of ANZ include the Southern Ocean and, more particularly, the Great Australian Bight, also identified as a potential moisture source for polar ARs reaching East Antarctica (Pohl et al., 2021a). These events also tend to be more frequent during the austral winter season, when the mid-latitude general circulation increases in strength. Thus, whether the detected moisture transport events reaching southern ANZ do correspond to ARs could be questioned. This issue is of importance, since the southern mid-latitudes correspond to one of the regions of largest AR development worldwide according to most AR detection schemes used in the ARTMIP project (Marquardt Collow et al., 2022). Algorithms excluding zonal IVT (e.g., Wille et al., 2021) lead to very different results in these regions. The difference could be meaningful for southern ANZ, but also the southernmost parts of South America, that is, the only major landmasses present at these latitudes.

Our results also suggest that the available moisture in the subtropical regions east of Australia could be a key variable to include in future studies, especially for the northern parts of ANZ. The question of the moisture sources for ARs could be addressed for example, by using back trajectories or Lagrangian approaches—as already indicated by Kingston and McMecking (2015) for flooding events in the Southern Alps. Latent heat fluxes at the interface between atmosphere and oceans (e.g., over Tasman and Coral seas) or continent (Australia) are intuitive candidates that could favor increased moisture in the lower troposphere, more likely to lead to AR formations. More generally, convective activity in the tropical to subtropical latitudes (e.g., in the vicinity of the nearby South Pacific Convergence Zone) could be a key parameter to consider in future work. By determining the available moisture ready to

be advected poleward, it could contribute to drive AR occurrence in the middle to high southern latitudes (e.g., Clem et al., 2022). Of particular interest could be the analysis of the influence of the Madden-Julian Oscillation (C. Zhang, 2005), since this near-global mode of variability is of major importance to organize large-scale convection in the tropics, and has been shown to modulate WT occurrence over ANZ (Fauchereau et al., 2016). How MJO and WTs add influence to drive AR development remains however to be assessed.

Last but not least, this work solely analyzed the synoptic scale, at which both WTs and ARs develop and interact. However, in the mid-latitudes of the Southern Hemisphere, atmospheric circulations strongly varied and evolved since the early 20th century (Fogt et al., 2009; Polvani et al., 2011; Thompson & Solomon, 2002), at various timescales spanning from interannual to multi-decadal (L'Heureux & Thompson, 2006; Oliveira et al., 2013). Such changes are further projected for the future decades under ongoing climate change (Arblaster et al., 2011; Perlwitz, 2011; Zheng et al., 2013): WTs (Gibson et al., 2016; Parsons et al., 2014) and ARs (Espinoza et al., 2018; Ma et al., 2020) themselves will also show gradually-evolving properties under increasing greenhouse gas concentrations. How these lower frequencies affect both WTs and ARs over the region is a major question to address. How changes in the atmospheric and climate dynamics (Sansom & Renwick, 2007) could combine their influence to the so-called Clausius-Clapeyron scaling (Betts & Harshvardhan, 1987; Kharin et al., 2007; Muller et al., 2011; O'Gorman & Schneider, 2009; Pall et al., 2007; Trenberth et al., 2003; Westra et al., 2014) to modify precipitation amounts, especially wet extremes at daily and sub-daily timescales, is another subject of concern for the local societies and territories. Further work is strongly needed to cast light on these subjects and help adapt to ever increasing changes in the local, regional and global climate.

Data Availability Statement

ERA5 data (Hersbach et al., 2020) can be retrieved from <https://cds.climate.copernicus.eu/cdsapp#!/search?type=dataset&text=era5>. The AR catalogs from the ARTMIP (<https://www.cgd.ucar.edu/projects/artmip>) Tier2 (Marquardt Collow et al., 2022) are available at <https://zenodo.org/record/5773269#.Y4Ci4-zMJGA>. AR detection is based on the algorithm originally introduced in Guan and Waliser (2015), refined in Guan et al. (2018), and further enhanced in Guan and Waliser (2019). Weather types and their descriptors (P21) are available at https://pohlben.files.wordpress.com/2022/02/ktdescriptors_era5.xlsx and https://pohlben.files.wordpress.com/2022/02/ktdescriptors_ncep.xlsx. VCSN data (Tait & Turner, 2005; Tait et al., 2006, 2012) can be retrieved from the NIWA website at <https://niwa.co.nz/climate/our-services/virtual-climate-stations>.

References

- Ackerley, D., Lorrey, A., Renwick, J. A., Phipps, S. J., Wagner, S., Dean, S., et al. (2011). Using synoptic type analysis to understand New Zealand climate during the Mid-Holocene. *Climate of the Past*, 7(4), 1189–1207. <https://doi.org/10.5194/cp-7-1189-2011>
- Arblaster, J. M., Meehl, G. A., & Karoly, D. J. (2011). Future climate change in the Southern Hemisphere: Competing effects of ozone and greenhouse gases. *Geophysical Research Letters*, 38(2), L02701. <https://doi.org/10.1029/2010GL045384>
- Bennet, M. J., & Kingston, D. G. (2022). Spatial patterns of atmospheric vapour transport and their connection to drought in New Zealand. *International Journal of Climatology*, 42(March 2021), 1–21. <https://doi.org/10.1002/joc.7554>
- Betts, A. K., & Harshvardhan (1987). Thermodynamic constraint on the cloud liquid water feedback in climate models. *Journal of Geophysical Research*, 92(D7), 8483–8485. <https://doi.org/10.1029/jd092id07p08483>
- Clem, K. R., Bozkurt, D., Kennett, D., King, J. C., & Turner, J. (2022). Central tropical Pacific convection drives extreme high temperatures and surface melt on the Larsen C Ice Shelf, Antarctic Peninsula. *Nature Communications*, 13(1), 3906. <https://doi.org/10.1038/s41467-022-31119-4>
- Coggins, J. H., Parsons, S., & Schiel, D. (2016). An assessment of the ocean wave climate of New Zealand as represented in Kidson's synoptic types. *International Journal of Climatology*, 36(6), 2481–2496. <https://doi.org/10.1002/joc.4507>
- Cullen, N. J., Gibson, P. B., Mölg, T., Conway, J. P., Sirguey, P., & Kingston, D. G. (2019). The influence of weather systems in controlling mass balance in the southern Alps of New Zealand. *Journal of Geophysical Research: Atmospheres*, 124(8), 4514–4529. <https://doi.org/10.1029/2018JD030052>
- Dravitzki, S., & McGregor, J. (2011). Extreme precipitation of the Waikato region, New Zealand. *International Journal of Climatology*, 31(12), 1803–1812. <https://doi.org/10.1002/joc.2189>
- Eiras-Barca, J., Lorenzo, N., Taboada, J., Robles, A., & Miguez-Macho, G. (2018). On the relationship between atmospheric rivers, weather types and floods in Galicia (NW Spain). *Natural Hazards and Earth System Sciences*, 18(6), 1633–1645. <https://doi.org/10.5194/nhess-18-1633-2018>
- Espinoza, V., Waliser, D. E., Guan, B., Lavers, D. A., & Ralph, F. M. (2018). Global analysis of climate change projection effects on atmospheric rivers. *Geophysical Research Letters*, 45(9), 4299–4308. <https://doi.org/10.1029/2017GL076968>
- Fauchereau, N., Pohl, B., & Lorrey, A. (2016). Extratropical impacts of the Madden-Julian oscillation over New Zealand from a weather regime perspective. *Journal of Climate*, 29(6), 2161–2175. <https://doi.org/10.1175/JCLI-D-15-0152.1>
- Fish, M. A., Wilson, A. M., & Ralph, F. M. (2019). Atmospheric river families: Definition and associated synoptic conditions. *Journal of Hydro-meteorology*, 20(10), 2091–2108. <https://doi.org/10.1175/JHM-D-18-0217.1>
- Fogt, R. L., Perlwitz, J., Monaghan, A. J., Bromwich, D. H., Jones, J. M., & Marshall, G. J. (2009). Historical SAM variability. Part II: Twentieth-century variability and trends from reconstructions, observations, and the IPCC AR4 models. *Journal of Climate*, 22(20), 5346–5365. <https://doi.org/10.1175/2009JCLI2786.1>

Acknowledgments

Three anonymous reviewers are thanked for their constructive comments that helped improve the text and the figures of this article. This study is a contribution to the International Research Programme VinAdapt funded by France and New Zealand, and sea4seas project funded by the University of Burgundy. BP and JW also acknowledge support from the Agence Nationale de la Recherche project, ANR-20-CE01-0013 (ARCA). NF was supported by the NIWA Strategic Science Investment Fund project “Climate Present and Past.” The authors thank Prof. James Renwick for making the original Kidson type distribution available and for updating it over the recent years. All analyses were made with python (libraries numpy, pandas, scipy, sklearn, math, matplotlib, cartopy, seaborn, netCDF4), the developers of which are thanked. Calculations were performed using HPC resources from DNUM CCUB (Centre de Calcul de l'Université de Bourgogne).

- Gibson, P. B., Perkins-Kirkpatrick, S. E., & Renwick, J. A. (2016). Projected changes in synoptic weather patterns over New Zealand examined through self-organizing maps. *International Journal of Climatology*, 36(January), 3934–3948. <https://doi.org/10.1002/joc.4604>
- Gimeno, L., Algarra, I., Eiras-Barca, J., Ramos, A. M., & Nieto, R. (2021). Atmospheric river, a term encompassing different meteorological patterns. *Wiley Interdisciplinary Reviews: Water*, 8(6), e1558. <https://doi.org/10.1002/wat2.1558>
- Gorodetskaya, I. V., Tsukernik, M., Claes, K., Ralph, M. F., Neff, W. D., & Van Lipzig, N. P. M. (2014). The role of atmospheric rivers in anomalous snow accumulation in East Antarctica. *Geophysical Research Letters*, 41(17), 6199–6206. <https://doi.org/10.1002/2014GL060881>
- Guan, B., & Waliser, D. E. (2015). Detection of atmospheric rivers: Evaluation and application of an algorithm for global studies [Software]. *Journal of Geophysical Research: Atmospheres*, 120(24), 12514–12535. <https://doi.org/10.1002/2015JD024257>
- Guan, B., & Waliser, D. E. (2019). Tracking atmospheric rivers globally: Spatial distributions and temporal evolution of life cycle characteristics [Software]. *Journal of Geophysical Research: Atmospheres*, 124(23), 12523–12552. <https://doi.org/10.1029/2019JD031205>
- Guan, B., Waliser, D. E., & Ralph, F. M. (2018). An intercomparison between reanalysis and dropsonde observations of the total water vapor transport in individual atmospheric rivers [Dataset]. *Journal of Hydrometeorology*, 19(2), 321–337. <https://doi.org/10.1175/JHM-D-17-0114.1>
- Guo, Y., Shinoda, T., Guan, B., Waliser, D. E., & Chang, E. K. M. (2020). Statistical relationship between atmospheric rivers and extratropical cyclones and anticyclones. *Journal of Climate*, 33(18), 7817–7834. <https://doi.org/10.1175/JCLI-D-19-0126.1>
- Hersbach, H., Bell, B., Berrisford, P., Hirahara, S., Horányi, A., Muñoz-Sabater, J., et al. (2020). The ERA5 global reanalysis [Dataset]. *Quarterly Journal of the Royal Meteorological Society*, 146(730), 1999–2049. <https://doi.org/10.1002/qj.3803>
- Hoskins, B. J., McIntyre, M. E., & Robertson, A. W. (1985). On the use and significance of isentropic potential vorticity maps. *Quarterly Journal of the Royal Meteorological Society*, 111(470), 877–946. <https://doi.org/10.1002/qj.49711146602>
- Jiang, N., Dirks, K. N., & Luo, K. (2013). Classification of synoptic weather types using the self-organising map and its application to climate and air quality data visualisation. *Weather and Climate*, 33, 52–75. <https://doi.org/10.2307/26169737>
- Jobst, A. M., Kingston, D. G., & Cullen, N. J. (2018). High resolution precipitation fields for the Clutha catchment. *Weather and Climate*, 38(1), 2–15. <https://doi.org/10.2307/26779360>
- Kalnay, E., Kanamitsu, M., Kistler, R., Collins, W., Deaven, D., Gandin, L., et al. (1996). The NCEP/NCAR 40-year reanalysis project [Dataset]. *Bulletin of the American Meteorological Society*, 77(3), 437–471. [https://doi.org/10.1175/1520-0477\(1996\)077<0437:tmyrp>2.0.co;2](https://doi.org/10.1175/1520-0477(1996)077<0437:tmyrp>2.0.co;2)
- Kharin, V. V., Zwiers, F. W., Zhang, X., & Hegerl, G. C. (2007). Changes in temperature and precipitation extremes in the IPCC ensemble of global coupled model simulations. *Journal of Climate*, 20(8), 1419–1444. <https://doi.org/10.1175/JCLI4066.1>
- Kidson, J. W. (2000). An Analysis of New Zealand synoptic types and their use in defining weather regimes. *International Journal of Climatology*, 20(3), 299–316. [https://doi.org/10.1002/\(sici\)1097-0088\(20000315\)20:3<299::aid-joc474>3.0.co;2-b](https://doi.org/10.1002/(sici)1097-0088(20000315)20:3<299::aid-joc474>3.0.co;2-b)
- Kingston, D. G., Lavers, D. A., & Hannah, D. M. (2016). Floods in the southern Alps of New Zealand: The importance of atmospheric rivers. *Hydrological Processes*, 30(26), 5063–5070. <https://doi.org/10.1002/hyp.10982>
- Kingston, D. G., Lavers, D. A., & Hannah, D. M. (2022). Characteristics and large-scale drivers of atmospheric rivers associated with extreme floods in New Zealand. *International Journal of Climatology*, 42(5), 3208–3224. <https://doi.org/10.1002/joc.7415>
- Kingston, D. G., & McMecking, J. (2015). Precipitation delivery trajectories associated with extreme river flow for the Waitaki River, New Zealand. *IAHS-AISH Proceedings and Reports*, 369, 19–24. <https://doi.org/10.5194/piahs-369-19-2015>
- L'Heureux, M. L., & Thompson, D. W. J. (2006). Observed relationships between the El-Niño-Southern oscillation and the extratropical zonal-mean circulation. *Journal of Climate*, 19(1), 276–287. <https://doi.org/10.1175/JCLI3617.1>
- Little, K., Kingston, D. G., Cullen, N. J., & Gibson, P. B. (2019). The role of atmospheric rivers for extreme ablation and snowfall events in the southern Alps of New Zealand. *Geophysical Research Letters*, 46(5), 2761–2771. <https://doi.org/10.1029/2018GL081669>
- Lorrey, A. M., Fauchereau, N., Stanton, C., Chappell, P., Phipps, S., Mackintosh, A., et al. (2014). The Little Ice Age climate of New Zealand reconstructed from southern Alps cirque glaciers: A synoptic type approach. *Climate Dynamics*, 42(11–12), 3039–3060. <https://doi.org/10.1007/s00382-013-1876-8>
- Lorrey, A. M., Fowler, A. M., & Salinger, J. (2007). Regional climate regime classification as a qualitative tool for interpreting multi-proxy palaeoclimate data spatial patterns: A New Zealand case study. *Palaeogeography, Palaeoclimatology, Palaeoecology*, 253(3–4), 407–433. <https://doi.org/10.1016/j.palaeo.2007.06.011>
- Lorrey, A. M., Vandergoes, M., Almond, P., Renwick, J., Stephens, T., Bostock, H., et al. (2012). Palaeocirculation across New Zealand during the last glacial maximum at ~21 ka. *Quaternary Science Reviews*, 36, 189–213. <https://doi.org/10.1016/j.quascirev.2011.09.025>
- Lorrey, A. M., Williams, P., Salinger, J., Martin, T., Palmer, J., Fowler, A., et al. (2008). Speleothem stable isotope records interpreted within a multi-proxy framework and implications for New Zealand palaeoclimate reconstruction. *Quaternary International*, 187(1), 52–75. <https://doi.org/10.1016/j.quaint.2007.09.039>
- Ma, W., Chen, G., & Guan, B. (2020). Poleward shift of atmospheric rivers in the southern Hemisphere in recent decades. *Geophysical Research Letters*, 47(21), e2020GL089934. <https://doi.org/10.1029/2020GL089934>
- Madonna, E., Wernli, H., Joos, H., & Martius, O. (2014). Warm conveyor belts in the ERA-Interim Dataset (1979–2010). Part I: Climatology and potential vorticity evolution. *Journal of Climate*, 27(1), 3–26. <https://doi.org/10.1175/JCLI-D-12-00720.1>
- Marquardt Collow, A. B., Shields, C. A., Guan, B., Kim, S., Lora, J. M., McClenny, E. E., et al. (2022). An overview of ARTMIP's tier 2 reanalysis intercomparison: Uncertainty in the detection of atmospheric rivers and their associated precipitation [Dataset]. *Journal of Geophysical Research: Atmospheres*, 127(8), e2021JD036155. <https://doi.org/10.1029/2021jd036155>
- Mason, E. G., Salekin, S., & Morgenroth, J. A. (2017). Comparison between meteorological data from the New Zealand National Institute of Water and Atmospheric Research (NIWA) and data from independent meteorological stations. *New Zealand Journal of Forestry Science*, 47(7), 7. <https://doi.org/10.1186/s40490-017-0088-0>
- Muller, C. J., O'Gorman, P. A., & Back, L. E. (2011). Intensification of precipitation extremes with warming in a cloud-resolving model. *Journal of Climate*, 24(11), 2784–2800. <https://doi.org/10.1175/2011JCLI3876.1>
- O'Gorman, P. A., & Schneider, T. (2009). Scaling of precipitation extremes over a wide range of climates simulated with an idealized GCM. *Journal of Climate*, 22(21), 5676–5685. <https://doi.org/10.1175/2009JCLI2701.1>
- Oliveira, F. M. N. M., V Carvalho, L. M., & Ambrizzi, T. T. (2013). A new climatology for Southern Hemisphere blockings in the winter and the combined effect of ENSO and SAM phases. *International Journal of Climatology*, 34(5), 1676–1692. <https://doi.org/10.1002/joc.3795>
- Pall, P., Allen, M. R., & Stone, D. A. (2007). Testing the Clausius-Clapeyron constraint on changes in extreme precipitation under CO₂ warming. *Climate Dynamics*, 28(4), 351–363. <https://doi.org/10.1007/s00382-006-0180-2>
- Parsons, S., McDonald, A. J., & Renwick, J. A. (2014). The use of synoptic climatology with general circulation model output over New Zealand. *International Journal of Climatology*, 34(12), 3426–3439. <https://doi.org/10.1002/joc.3919>
- Perlwitz, J. (2011). Tug of war on the jet stream. *Nature Climate Change*, 1(1), 29–31. <https://doi.org/10.1038/nclimate1065>
- Pfahl, S., Schwierz, C., Croci-Maspoli, M., Grams, C. M., & Wernli, H. (2015). Importance of latent heat release in ascending air streams for atmospheric blocking. *Nature Geoscience*, 8(8), 610–614. <https://doi.org/10.1038/ngeo2487>

- Pohl, B., Favier, V., Wille, J., Udy, D. G., Vance, T. R., Pergaud, J., et al. (2021a). Relationship between weather regimes and atmospheric rivers in East Antarctica. *Journal of Geophysical Research: Atmospheres*, *126*(24), e2021JD035294. <https://doi.org/10.1029/2021JD035294>
- Pohl, B., Lorrey, A., Sturman, A., Quénol, H., Renwick, J., Fauchereau, N., & Pergaud, J. (2021b). "Beyond weather regimes": Descriptors monitoring atmospheric centers of action—a case study for aotearoa New Zealand [Dataset]. *Journal of Climate*, *34*(20), 8341–8360. <https://doi.org/10.1175/JCLI-D-21-0102.1>
- Pohl, B., Saucède, T., Favier, V., Pergaud, J., Verfaillie, D., Féral, J.-P., et al. (2021c). Recent climate variability around the Kerguelen Islands (Southern Ocean) seen through weather regimes. *Journal of Applied Meteorology and Climatology*, *60*, 711–731. <https://doi.org/10.1175/jamc-d-20-0255.1>
- Pohl, B., Sturman, A., Renwick, J., Quénol, H., Fauchereau, N., Lorrey, A., & Pergaud, J. (2023). Precipitation and temperature anomalies over Aotearoa New Zealand analysed by weather types and descriptors of atmospheric centres of action. *International Journal of Climatology*, *43*(1), 331–353. <https://doi.org/10.1002/joc.7762>
- Polvani, L. M., Waugh, D. W., Correa, G. J. P., & Son, S.-W. (2011). Stratospheric ozone depletion: The main driver of twentieth-century atmospheric circulation changes in the southern Hemisphere. *Journal of Climate*, *24*(3), 795–812. <https://doi.org/10.1175/2010JCLI3772.1>
- Porhemmat, R., Purdie, H., Zavar-Reza, P., Zammit, C., & Kerr, T. (2021a). The influence of atmospheric circulation patterns during large snowfall events in New Zealand's Southern Alps. *International Journal of Climatology*, *41*(4), 2397–2417. <https://doi.org/10.1002/joc.6966>
- Porhemmat, R., Purdie, H., Zavar-Reza, P., Zammit, C., & Kerr, T. (2021b). Moisture transport during large snowfall events in the New Zealand southern Alps: The role of atmospheric rivers. *Journal of Hydrometeorology*, *22*(2), 425–444. <https://doi.org/10.1175/jhm-d-20-0044.1>
- Prince, H. D., Cullen, N. J., Gibson, P. B., Conway, J., & Kingston, D. G. (2021a). A climatology of atmospheric rivers in New Zealand. *Journal of Climate*, *34*(11), 4383–4402. <https://doi.org/10.1175/JCLI-D-20-0664.1>
- Prince, H. D., Gibson, P. B., DeFlorio, M. J., Corringham, T. W., Cobb, A., Guan, B., et al. (2021b). Genesis locations of the costliest atmospheric rivers impacting the western United States. *Geophysical Research Letters*, *48*(20), e2021GL093947. <https://doi.org/10.1029/2021GL093947>
- Ralph, F. M., Dettinger, M., Lavers, D., Gorodetskaya, I. V., Martin, A., Viale, M., et al. (2017). Atmospheric rivers emerge as a global science and applications focus. *Bulletin of the American Meteorological Society*, *98*(9), 1969–1973. <https://doi.org/10.1175/BAMS-D-16-0262.1>
- Ralph, F. M., Dettinger, M. D., Cairns, M. M., Galarneau, T. J., & Eylander, J. (2018). Defining "Atmospheric river": How the glossary of meteorology helped resolve a debate. *Bulletin of the American Meteorological Society*, *99*(4), 837–839. <https://doi.org/10.1175/BAMS-D-17-0157.1>
- Ralph, F. M., Rutz, J. J., Cordeira, J. M., Dettinger, M., Anderson, M., Reynolds, D., et al. (2019). A scale to characterize the strength and impacts of atmospheric rivers. *Bulletin of the American Meteorological Society*, *100*(2), 269–289. <https://doi.org/10.1175/BAMS-D-18-0023.1>
- Reid, K. J., King, A. D., Lane, T. P., & Hudson, D. (2022). Tropical, subtropical and extratropical atmospheric rivers in the Australian region. *Journal of Climate*, *35*(9), 2697–2708. <https://doi.org/10.1175/jcli-d-21-0606.1>
- Reid, K. J., Rosier, S. M., Harrington, L. J., King, A. D., & Lane, T. P. (2021). Extreme rainfall in New Zealand and its association with atmospheric rivers. *Environmental Research Letters*, *16*(4), 044012. <https://doi.org/10.1088/1748-9326/abea60>
- Renwick, J. A. (2011). Kidson's synoptic weather types and surface climate variability over New Zealand. *Weather and Climate*, *31*, 3–23. <https://doi.org/10.2307/26169715>
- Salinger, M. J., Diamond, H. J., Behrens, E., Fernandez, D., Fitzharris, B. B., Herold, N., et al. (2020). Unparalleled coupled ocean-atmosphere summer heatwaves in the New Zealand region: Drivers, mechanisms and impacts. *Climate Change*, *162*(2), 485–506. <https://doi.org/10.1007/s10584-020-02730-5>
- Sansom, J., & Renwick, J. A. (2007). Climate change scenarios for New Zealand rainfall. *Journal of Applied Meteorology and Climatology*, *46*(5), 573–590. <https://doi.org/10.1175/JAM2491.1>
- Shu, J., Shamseldin, A. Y., & Weller, E. (2021). The impact of atmospheric rivers on rainfall in New Zealand. *Scientific Reports*, *11*(1), 1–11. <https://doi.org/10.1038/s41598-021-85297-0>
- Smith, W., Davies-Colley, C., Mackay, A., & Bankoff, G. (2011). Social impact of the 2004 Manawatu floods and the "hollowing out" of rural New Zealand. *Disasters*, *35*(3), 540–553. <https://doi.org/10.1111/j.1467-7717.2011.01228.x>
- Sodemann, H., & Stohl, A. (2013). Moisture origin and meridional transport in atmospheric rivers and their association with multiple cyclones. *Monthly Weather Review*, *141*(8), 2850–2868. <https://doi.org/10.1175/MWR-D-12-00256.1>
- Tait, A., Henderson, R., Turner, R., & Zheng, X. (2006). Thin plate smoothing spline interpolation of daily rainfall for New Zealand using a climatological rainfall surface [Dataset]. *International Journal of Climatology*, *26*(14), 2097–2115. <https://doi.org/10.1002/joc.1350>
- Tait, A., Sturman, J., & Clark, M. (2012). An assessment of the accuracy of interpolated daily rainfall for New Zealand. *Journal of Hydrology*, *51*(1), 25–44.
- Tait, A., & Turner, R. (2005). Generating multiyear gridded daily rainfall over New Zealand [Dataset]. *Journal of Applied Meteorology*, *44*(9), 1315–1323. <https://doi.org/10.1175/JAM2279.1>
- Terpstra, A., V. Gorodetskaya, I., & Sodemann, H. (2021). Linking sub-tropical evaporation and extreme precipitation over East Antarctica: An atmospheric river case study. *Journal of Geophysical Research: Atmospheres*, *126*(9), e2020JD033617. <https://doi.org/10.1029/2020JD033617>
- Thompson, D. W. J., & Solomon, S. (2002). Interpretation of recent Southern Hemisphere climate change. *Science*, *296*(5569), 895–899. <https://doi.org/10.1126/science.1069270>
- Trenberth, K. E., Dai, A., Rasmussen, R. M., & Parsons, D. B. (2003). The changing character of precipitation. *Bulletin of the American Meteorological Society*, *84*(9), 1205–1217. <https://doi.org/10.1175/BAMS-84-9-1205>
- Westra, S., Fowler, H. J., Evans, J. P., V. Alexander, L., Berg, P., Johnson, F., et al. (2014). Future changes to the intensity and frequency of short-duration extreme rainfall. *Reviews of Geophysics*, *52*(3), 522–555. <https://doi.org/10.1002/2014RG000464>
- Wille, J. D., Favier, V., Gorodetskaya, I., Agosta, C., Kittel, C., Beeman, J. C., et al. (2021). Antarctic atmospheric river climatology and precipitation impacts. *Journal of Geophysical Research: Atmospheres*, *126*(8), e2020JD033788. <https://doi.org/10.1029/2020jd033788>
- Wille, J. D., Favier, V., Jourdain, N. C., Kittel, C., Turton, J. V., Agosta, C., et al. (2022). Intense atmospheric rivers can weaken ice shelf stability at the Antarctic Peninsula. *Communications Earth & Environment*, *3*(1), 90. <https://doi.org/10.1038/s43247-022-00422-9>
- Woollings, T., Barriopedro, D., Methven, J., Son, S. W., Martius, O., Harvey, B., et al. (2018). Blocking and its response to climate change. *Current Climate Change Reports*, *4*(3), 287–300. <https://doi.org/10.1007/s40641-018-0108-z>
- Zhang, C. (2005). Madden-Julian oscillation. *Reviews of Geophysics*, *43*(2), RG2003. <https://doi.org/10.1029/2004RG000158>
- Zhang, Z., Ralph, F. M., & Zheng, M. (2019). The relationship between extratropical cyclone strength and Atmospheric River intensity and position. *Geophysical Research Letters*, *46*(3), 1814–1823. <https://doi.org/10.1029/2018GL079071>
- Zheng, F., Li, J., Clark, R. T., & Nnamchi, H. C. (2013). Simulation and projection of the Southern Hemisphere annular mode in CMIP5 models. *Journal of Climate*, *26*(24), 9860–9879. <https://doi.org/10.1175/JCLI-D-13-00204.1>
- Zhu, Y., & Newell, R. E. (1994). Atmospheric rivers and bombs. *Geophysical Research Letters*, *21*(18), 1999–2002. <https://doi.org/10.1029/94GL01710>